MODELLING OF FLARES ON LATE-TYPE STARS

D.GARCIA ALVAREZ
Armagh Observatory, College Hill, Armagh BT61 9DG, N. Ireland
email: dga@star.arm.ac.uk

ABSTRACT. Stellar flare research is an exciting and rapidly developing field of astrophysics. The Sun is an invaluable proving ground to test predictions of flare theories and to develop analytical techniques for future stellar applications, because the lack of spatial resolution for stellar flares pushes us to extrapolate models of solar flares to the stellar situation. Stellar flares can sometimes be several orders of magnitude more energetic than their solar counterparts, which may suggest that new phenomena are taking place which are not observed on the Sun. Because of widely different energy ranges and atmospheric properties, the investigation of stellar flares is seen as a potential breakthrough in our understanding of flares as a whole. Because flarelike physical processes occur in diverse astrophysically interesting regimes, the field of solar and stellar flares, and therefore, their modelling can serve as an astrophysical touchstone.

1. INTRODUCTION

Stellar flare research is an exciting and rapidly developing field of astrophysics. Flares are important to astrophysics because they originate in out-of-equilibrium magnetic field-plasma interactions rather than in gravitational, thermonuclear, or radiative processes in near equilibrium. Flare stars constitute about ~90% of the stars in the Galaxy. The Sun is an invaluable proving ground to test predictions of flare theories and to develop analytical techniques for future stellar applications, because the lack of spatial resolution for stellar flares pushes us to extrapolate models of solar flares to the stellar situation.

Stellar flares are believed to be solar type events during which a large amount of energy may be released in a short interval of time (up to 3×10^{36} ergs, Haisch et al 1991), radiating at almost all frequencies in the electromagnetic spectrum. However, the magnetic energy release and conversion has never been directly observed. The relative increase of the stellar brightness might reach 8 magnitudes in the Jonhson U-band for the largest flares. Such a change in the star radiation field modifies drastically the atmospheric properties over large areas, from photospheric to coronal layers. These flares can sometimes be several orders of magnitude more energetic than their solar counterparts, which may suggest that new phenomena are taking place which are not observed on the Sun.

Because of widely different energy ranges and atmospheric properties, the investigation of stellar flares is seen as a potential breakthrough in our understanding of flares as a whole. For instance, results by Houdebine (1992) indicate that heating propagates down to low photospheric levels, to densities higher than $10^{16} cm^{-3}$, and that electrons with energies in the MeV range are required to attain such depth. Because flarelike physical processes occur in diverse astrophysically interesting regimes, the field of solar and stellar flares, and therefore, their modelling can serve as an astrophysical touchstone.

2. HISTORY OF FLARES

2.1. Solar Flares

Solar flares were discovered by Carrington and Hodgson's 1859 observations (Figure 1). Prior to the space era, virtually all flare observations involved photography in chromospheric lines: commonly Hα at 6563$\AA$, other Balmer lines, HeI D3, CaII H&K, MgI b, and Na D. A major discovery was that flares occur along the magnetic neutral line. The three Skylab missions in 1973-74 opened up the UV and X-ray window, and demonstrated that the primary flare was not in the chomosphere.

2.2. Stellar Flares

In 1948 a spectrogram of the dMe dwarf star L726-8 by Joy & Humason (1949) revealed both line emission and continuum enhancement amounting to a change of about one magnitude. Thus began a long period of flare studies directed toward photometry of dKe/dMe UV Ceti-type stars in the U and B bands. Studies concentrated on flare ocurrence versus energy for different stars, measurement of flare colors and their temporal evolution, and recombination modeling of the optical radiation.

Stellar radio flares also turned out to be unexpectedly bright, but studies of this type languished until the mid 1970s when interferometric techniques and the VLA came into use. When the EUV/X-ray window finally opened on the stellar side to reveal the high energy flare (Haisch et al 1977), solar and stellar studies at last emerged from their mutual isolation and began the current trend of cross-fertilization.

3. FLARE STARS

3.1. Flares stars in H-R diagram

The "clasical" flare stars are the UV Ceti stars, which are main sequence (MS) stars of spectral type later than ~ K5Ve. Their characteristic property is rapid rotation, which, in combination with a deep convection zone, generates efficient dynamo activity. As in the Sun, the resulting magnetic fields rise through

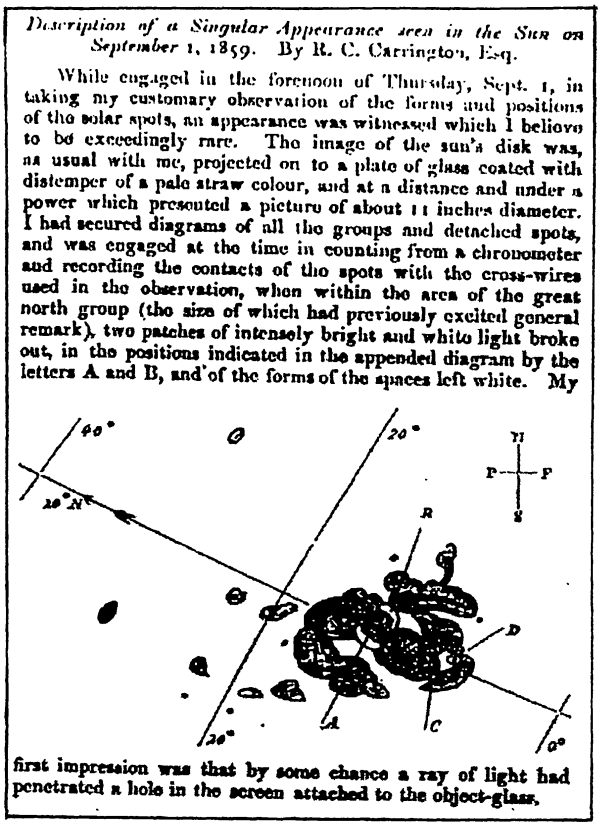

Description of a Singular Appearance seen in the Sun on September 1, 1859. By R. C. Carrington, Esq.

While engaged in the forenoon of Thursday, Sept. 1, in taking my customary observation of the forms and positions of the solar spots, an appearance was witnessed which I believe to be exceedingly rare. The image of the sun's disk was, as usual with me, projected on to a plate of glass coated with distemper of a pale straw colour, and at a distance and under a power which presented a picture of about 11 inches diameter. I had secured diagrams of all the groups and detached spots, and was engaged at the time in counting from a chronometer and recording the contacts of the spots with the cross-wires used in the observation, when within the area of the great north group (the size of which had previously excited general remark), two patches of intensely bright and white light broke out, in the positions indicated in the appended diagram by the letters A and B, and of the forms of the spaces left white. My

first impression was that by some chance a ray of light had penetrated a hole in the screen attached to the object-glass.

Fig. 1. The article in an early 1860 issue of Montly Notices announcing the discovery of a flare on the Sun

the convection zone and at the photosphere are locally intensified by surface convection into active regions, within which flares occur in stressed loop structures.

A second class of flare stars are the RS CVn stars. These are detached binaries with one evolved component normally forced into co-rotation with the orbital period by tidal interaction. The resulting rapid rotation, in combination with a deepening convective zone, results in dynamo-generated magnetic fields which produce flares in the same general manner as in the UV Cet stars. For a discussion of the UV Cet and RS CVn stars in comparison with the Sun in different wavelengths see Flares and Flashes (1994).

G dwarfs should flare if the Sun is typical, but, because of low optical contrast of a flare against the disk integrated flux, researchers could not directly observe such flares until Exosat measured a large flare on the active, rapidly rotating G0 V star π UMa. Flares are also found in a number of other kinds of objects. A literature search reveals flaring in many types of stars across the HR diagram as shown in Figure 2.

Among young stars, flaring has been reported on a few T Tauri stars, on members of young open clusters (eg. Pleiades and Orion), on stars on star formation regions, in stars close to

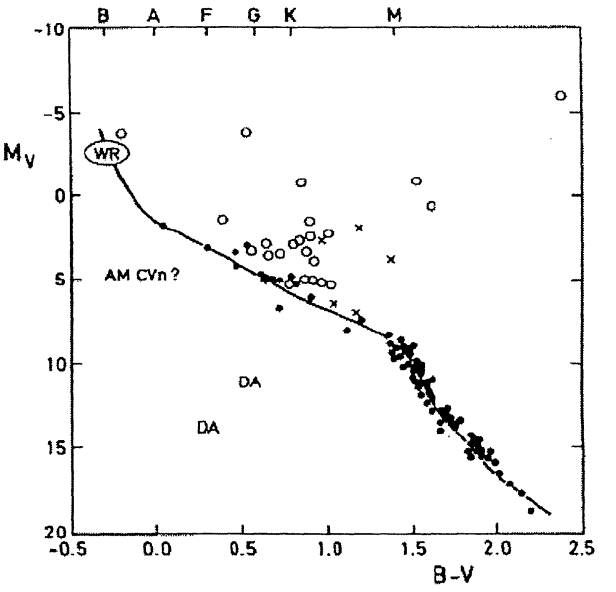

Fig. 2. Positions of some flaring objects in the HR-diagram (Pettersen 1989)

the main sequence and on post-T Tauri stars. On the Main Sequence we can find examples of flare stars in all spectral classes - from Wolf-Rayet stars and B stars to K and M dwarfs. Flares are also found on evolved objects: Algol and W UMa systems, late type giants and supergiants and systems containing white dwarfs.

The most extensive flare monitoring has been done for solar neighbourhood dKe and dMe stars and flare stars in various young clusters and aggregates, so most of our knowledge of flare characteristics comes from these observations. Individual stellar flares span considerable ranges in energy, amplitude and time-scale.

Flares weaker than 10^{27} ergs are seen on the intrinsically faintest stars with the brightest dKe stars showing flares of up to 10^{34} ergs and cluster flare stars and evolved stars showing flares of up to 10^{37} ergs (Pettersen 1989). Stars with less than about 50 recorded flares show a range in flare energy of 2-3 orders of magnitude, while stars with about 200 observed flares span 4-5 orders of magnitude in flare energy.

3.2. Flares on late-type stars

Flares on red dwarf stars have been studied for more than 50yr. The majority of impulsive flares are detected in the optical continuum and typically last from half a second or so to a few minutes, while powerful flares in the U-band with durations of some dozens of minutes have been observed on prototype flare stars. The duration of flares observed in Balmer lines is slighty longer than the flare optical continuum, and optical flare emission in the lines can last several hours (Hawley et al. 1995). The soft X-ray emission of flares on red dwarfs generally lasts not longer than 1 hour-a timescale and is thought to be de-

termined by the radiative cooling time of hot ($10^6 - 10^7$K or more) plasma (Pallavicini, Tagliaferri & Stella 1990), which in the standard of solar flare thick target heated chromosphere model is thought to be evaporated upward into high coronal loops by the impact of accelerated electrons and protons (Sturrock et al. 1986).

Because of limited sensitivity, most studies of activity in late-type stars have concentrated on the more active dMe stars which have large rates of radiative energy from almost all levels of their atmospheres.

Stellar flares on the red dwarfs are predominantly continuum events in terms of energy, but emission lines are enhanced before and well after the continuum component. Contrast effects on the brighter stars help to mask out the continuum and only very energetic flares are visible. Estimates from stellar flare data in other spectral regions suggest that roughly equal amounts of flare energy are emitted in the optical, UV and X-ray windows (Pettersen 1988).

4. LATE-TYPE STARS

Two thirds of the stars in the Milky Way are M dwarfs. Although their individual masses are small, they account, due to their large number, for half the total mass of main-sequence stars, or about 20% of the luminous mass of the galaxy. Apart from their intrinsic interest, the similarity between solar activity and M dwarf activity suggests that a comparative study can be very valuable for our understanding of phenomena like chromospheric and coronal heating, stellar activity and dynamos.

Among the M dwarfs, there is a well-known empirical distinction between two classes (dM and dMe) based on an optical criterion: dMe stars have $H\alpha$ in emission (a signature of a dense chromosphere (Cram & Mullan 1979), while dM stars have $H\alpha$ in absortion. Young et al. (1984) drew attention to a group of M dwarf stars with weak Hα absortion and suggested that these are examples of a class of late-type stars which is intermediate, in respect of its chromospheric activity, between the dM and the dMe stars. They suggested that such stars have chomospheres of electron density intermediate between the high densities of the dMe stars ($logN_e \approx 12 - 13cm^{-3}$) and the dM stars ($logN_e \approx 9.5 - 10.5cm^{-3}$).The dMe stars are highly active. The existence of a rotation-activity connection for the dMe stars suggests that dynamo operation is likely in these stars: magnetic fields (which creates the flares) must contribute significantly to atmospheric heating in such stars. On the other hand, the dM stars are less active, although by no means lacking in chromospheric heating or flares (Cram & Mullan 1979; Byrne 1981; Doyle et al. 1994).

dM stars and dMe stars can also be distinguished by means of an X-ray criterion. In terms of the mean surface flux of X-ray, dMe and dM stars form statistically significant distinct populations. Based on theoretical modeling of acoustic dissipation, coronal heating in dMe stars cannot be predominantly acoustic in nature. Active regions occupy no more than about 10% of the area of dM stars, and quiet regions occupy no more than about 50% of dMe stars.

The presence in dM and dMe stars of many atomic lines and molecular bandheads in absorption, proves the existence of a cool photosphere, whereas the fact that M dwarfs show an emission core in the Ca II resonance lines implies that they have a chromosphere. The difference between the spectra of dM and dMe stars is due to a different chromospheric structure as occurs in quiet and active regions on the Sun.

Evidence now exists indicating that the flare stars are the youngest stars among the M dwarfs, with youth being considered as a sufficient condition for low-mass stars to show flare activity (Rodonò 1986; Gurzadyan 1980).

M dwarfs occupy the lower end of the main sequence and are represented by the following mass luminosity relation

$$\frac{L}{L_\odot} \propto \left(\frac{M}{M_\odot}\right)^{2.2\pm0.2} \quad (1)$$

The masses of dM stars range from $0.7M_\odot$ down to the hydrogen ignition mass while their radii range from $1R_\odot$ to $0.15R_\odot$. For empirical correlations between global parameters of M dwarfs see Rodonò (1986).

Observations of late-type dwarfs show the existence of solar type atmospheres and activity. Emission reversals in the Ca II H&K and Mg II h&k lines are present in their spectra, as well as lines of highly ionized ions such as C II, C IV, Si IV, N V and others.

The photosphere is the part of the atmosphere where the temperature gradient is negative as one would expect in radiative equilibrium. This does not mean that non-radiative heating is not dissipated there, but it rather means that it is not enough to balance the large radiative losses, which are due to the large density and therefore can not force a temperature inversion. In the chromosphere the non-raditive heating rate is sufficient to force a gradual positive temperature gradient. Lines such as Ca II H&K, Mg II h&k, H I Balmer series, Fe II etc dominate the chromospheric losses. The transition region is inmediately above the chromosphere and is characterised by a very steep positive temperature gradient. Emission lines in the UV and EUV region dominate the radiative losses. The steep temperature gradient occurs because the low density makes the losses by radiation small compared with the energy input. Finally the corona has a small positive temperature gradient and is also heated by non-radiative processes. Cooling mechanisms for the corona include X-ray and EUV radiation, thermal conduction and energy loss by stellar wind.

5. TYPES OF FLARES

Exosat observations of flares stars revealed examples of two differents types of flares:

1. **Impulsive Flares** which are like solar compact flares.
2. **Long-Decay Flares** which are like solar two-ribbon flares.

The concept of Two-Ribbon vs Compact Flares has developed how a dichotomy between flares that are small in energy ($\sim 10^{30}ergs$), short in duration ($\sim 10^3 s$), and confined to a single loop (compact flares); and events that are more energetic ($\sim 10^{32}ergs$), of long duration ($\sim 10^4 s$), and involve the evolution and release of energy in an entire arcade of loops (two-ribbon flares). Compact flares always occur along magnetic neutral lines and either peak in the optical in less than 30s or continue to rise in brightness at a very rapid rate. Two ribbon flares are associated with filament eruptions and have multiple rises and dips in their light curves that may last for hours. It is useful to conceptualize the flare processes taking place in an energized single loop and to think of a two-ribbon

flare as a sequence of reconnections and energy releases taking place in higher and higher magnetic loops in an arcade triggering a series of compact flares. Examination of the Exosat data base revealed examples of stellar analogs for the two different types of flares-compact and two-ribbon- seen on the Sun. Impulsive flares, which are like solar compact flares, and long-decay flares, which are like solar two-ribbon flares, have both been found to occur on the same star.

One would like to trace all the energetic processes in a flare to some common origin likely to be localized at some unresolvably fine scale in the magnetic field. However, we are not yet sure that all possible energy routes have been identified. The largest solar flare ever studied involved $E \sim 2 \times 10^{32} ergs$, several large flares studied on dMe stars involved $E \sim 10^{34} ergs$. Even more energetic flares occur on the RS CVn stars, the total flare energy in the largest in this kind of stars may exceed $E \sim 10^{38} ergs$.

5.1. Phases of Flares

Generally flares can be divided into four phases:

1. **Preflare phase.**
2. **Impulsive phase**, which is part of the flash phase and during which the continuum radiation is the dominant source of energy loss, on also in the gradual phase.
3. **Main phase** or **Gradual Decay phase**, which up to now, is the main period amenable for the determination of the characteristic sizes of coronal structures, although in principle it only gives information about the flaring regions. There is five possible mechanisms for transporting energy from the corona to loop footpoints:
   (a) Thermal plasma with T$\geq 10^8$ K (i.e., so-called thermal model).
   (b) Fast electrons with energies ~10-100 keV.
   (c) Relativistic electrons.
   (d) Protons with energies $\leq$1 MeV.
   (e) Protons with energies $\geq$1 MeV.
4. **Late phase**, dominated by soft X-ray emission cooling the hot plasma, although even during this late phase there is likely to be some energy release (continued heating) taking place. Many other researchers however refer to the entire soft X-ray phase as the gradual phase, distinguishing only an impulsive and a gradual phase. On the stellar side, it has only been possible, because of wavelength and sesitivity limits, to observe the late phase in X-rays (Haisch 1989).

There exist no strict definitions of these phases. Also there are some flares with no impulsive phase (but rather a gradual enhancement of emission).

6. SPECTRAL RANGES OF FLARES

Flares produce emissions from γ-rays to the radio, each part revealing a different aspect, of these process. Thus is why simultaneous data taken at many wavelenghts are important (Figure 3). The upcoming generation of satellites missions (Chandra and XMM) will offer the possibility of a better understanding of X-ray emission.

6.1. UV

The far UV spectrum has been the subject of extensive investigations for the Sun, primarily because of its ability to

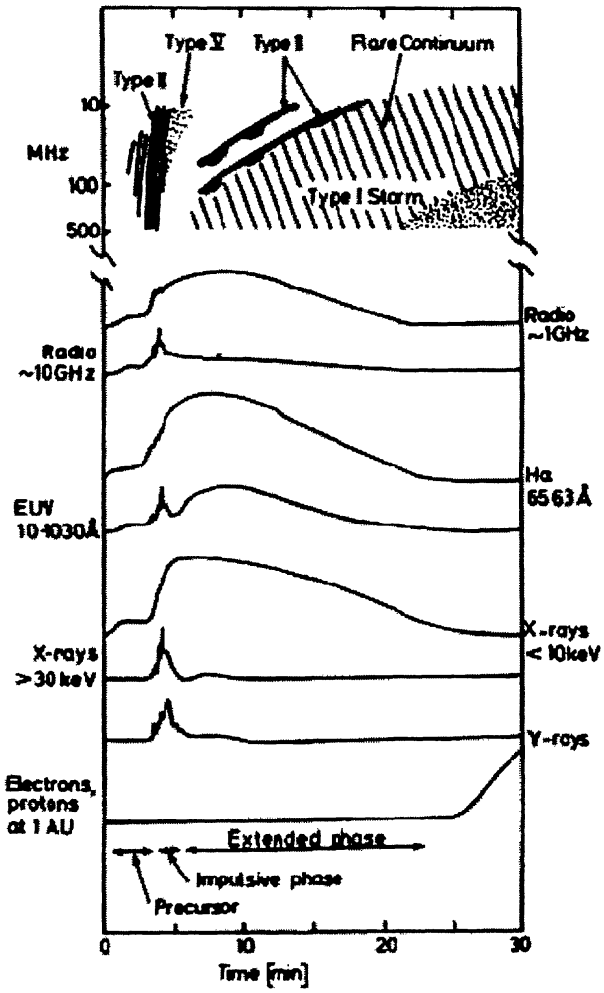

Fig. 3. Electromagnetic and particle radiation for a typical flare

diagnose the outer atmosphere from the temperature minimun (SiIλ1681, SiIλ1575, SiIλ1524, CIλ1098) to the transition region (HI Lyman) (Vernazza et al. 1981, Avrett 1985). As well as the far infra-red and millimeter continuum, it has proved more reliable in constraining the temperature minimum region than the CaII and MgII resonance lines (Vernazza et al. 1981). In other main sequence stars, the UV continuum emission of the atmosphere has not being analysed fully, probably because of the lack of observational constrain. We must acknowledge that apart from the Sun and despite considerable progress for instance in imaging techniques, extremely little is known about the physical properties of stellar inhomogeneities at low atmospheric levels such as dark and bright spots. There are a couple of important reasons however why one should have a detailed look at the UV continuum in active stars. First, the high contrast with the photospheric bakground is unique in late-type stars and its diagnostical potential is very high. Second, unlike the quiet Sun for which radiative cooling in spectral lines

is orders of magnitude larger than in the continuum, models that span over a large pressure range (e.g. flare models on the Sun,T Tauri stars) show that HI and H^- continua dominate the cooling from the temperature minimum to the transition region (Avrett 1986). Contrary to (usually recognized) main-sequence dwarfs, pre-main sequence objects, a class of stars which also displays magnetic activity of solar type, exhibit peculiar properties in the UV including a strong blue to EUV excess. The nature of this excess and its relation with surface magnetic fields are also ambiguous. Some models support a circumstellar origin whereas others place it at much lower levels, in the chromosphere and photosphere. In normal stellar atmospheres, there is a known long term disagreement between models based on CaII lines and the UV continuum for the Sun (Vernazza et al. 1981) and with MgII lines for M dwarfs (Giampapa et al. 1982). Houdebine et al. (1996) showed that a chromospheric/photospheric contribution to the UV excess is compulsory even if not dominant.

6.2. X-rays

While the solar analogy is almost universally accepted as the starting point for the modeling of stellar coronae, its scaling to the much higher activity levels seen in active stars is still a debated question. The Sun displays, even at the maximum of its 11 year cycle, a rather low level of activity, when compared to the most active stars; dMe dwarfs (flare stars) on the other hand exhibit quiescent activity levels which are up to three orders of magnitude higher (in terms of the surface flux) than the Sun at minimum, and still a factor of hundred higher when compared with the Sun at maximum.

The question of the scaling of the corona to higher X-ray luminosity is relevant to stellar evolution in general: higher-pressure structures imply larger contiement of magnetic fields, which in turn will have an influence on the convection region (magnetic fields modify the heat-transport capacity of the convective envelope), and thus on the structure of the star as such. High internal magnetic fields may even prevent a low-mass star from becoming fully convective. The structure of the magnetic field will also have an influence on the loss of angular momentum through magnetic braking, and thus again on the evolution of the internal structure of the star, as well as, on the depletion pattern of light elements (Ventura et al. 1998). Finally, the issue of whether the frequent and intense flares seen in very active stars are produced within closed coronal structures (as opposed to the production of intense flares in freely expanding plasmoids, i.e. large-scale coronal mass ejections) is relevant to the question of the contribution of the plentiful low-mass flare stars to the chemical evolution of our Galaxy.

There are several reasons that make the study of the coronal emission of the dMe stars a worthy while effort. First of all, their X-ray emission level - either expressed in terms of X-ray luminosity, L_X, or in terms of the X-ray luminosity scaled to the bolometric luminosity, L_X/L_{Bol} - makes them the most intense coronal emitters (with the only exception of the so-called active binaries, and of pre-main-sequence stars), hence they are a good test-bed for any proposed mechanism for the heating of stellar coronae. Their internal structure, reflected by their cool photospheres, should minimize any contribution by non-magnetic (acoustic) heating processes making it easier to pin point the characteristic features of the coronal magnetic heating mechanism and their relation to any kind of dynamo activity, either based on a scaled version of the solar $\alpha - \omega$ dynamo or on the more elusive turbulent dynamo (Durney et al. 1993) that has been suggested to be at work in the (almost) fully convective late dM stars (Stern et al. 1995). Another important issue is that of the transient activity, down to the "microflare" level, as an important contributor to the heating of dM coronae and the relation between this (micro)flaring activity and any dynamo action at work in the interior of these stars. Finally it is worthy while mentioning that dM stars are by far the most numerous of the coronal sources in our Galaxy, so that a better knowledge of their coronal spectra is important for any improvement in our capability to accurately predict the stellar contribution to the diffuse X-ray background.

6.3. Balmer Lines

Unlike most main sequence stars of G and K spectral types, M type stars show an unprecedented variety of Balmer line profiles (Figure 4). For very active stars, $H\alpha$ is strongly in emission with a weak self-reversal (Pagani et al. 1991) and an equivalent width usually in the range 1Å to 5Å. Other data sets, including M and K dwarfs or late M dwarfs, and modelling show this to be a normal characteristic of emission profiles formed in an optically thick chromosphere (Houdebine & Doyle 1994b). There are however a few exceptions to this rule. Others stars are believed to be of intermediate activity exhibit an almost zero $H\alpha$ equivalent width with inner wings in emission and an absortion core, while others (sometimes described as having a low activity level) show $H\alpha$ in absortion with an equivalent width from 0.7Å to zero (Panagi & Mathioudakis 1993). The latter type, the so-called "zero $H\alpha$ stars", are probably those showing the lowest level of magnetic activity, and their chromosphere (basal in character), if any, might be heated by acoustic waves (Doyle et al. 1994).

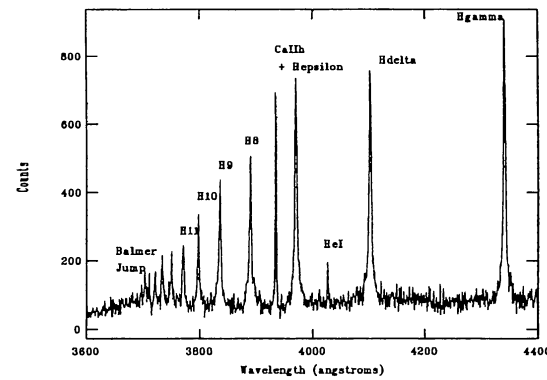

Fig. 4. Balmer emission and wing broadening, higher members of the Balmer series, and the emission of HeI line at 4026Å

The $H\alpha$ line source functions is controlled by the Balmer and Paschen continua in the solar and solar-like chromospheres of low and intermediate activity levels ($H\alpha$ in absortion) (Cram & Mullan 1985, Gebbie & Steinitz 1974). In such a chromosphere, its formation spreads from the phbtosphere to the mid-

dle or upper chromosphere. In M dwarf atmospheres however, the situation is somewhat different. The very low photospheric temperature implies a null or very weak photospheric contribution to the $H\alpha$ line (Cram & Giampapa 1987; Doyle et al. 1994) and the faint radiation field makes possible the collisional control of the line for a sufficient electron density (Fosbury 1974, Cram & Mullan 1979). Therefore, for dMe stellar chromospheres, it is a direct diagnostic of the chromospheric structure and pressure in the same way as other collisionally controlled lines; e.g. the CaII and MgII resonances lines.

6.3.1. Balmer Decrement

Balmer decrements (flux ratio of higher series members to $H\alpha$ have been used occasionally to derive plasma densities and temperatures in M dwarf chromospheres (Gershberg 1974; Gershberg & Luund 1975, Katsova 1990). Theoretical Balmer decrements can be calculated from:

$$\frac{F(H_i)}{F(H_\gamma)} = \frac{n_i A_{i2} h\nu_{i2} \beta_{i2}}{n_5 A_{52} h\nu_{52} \beta_{52}} \quad (2)$$

where n_i represents the population of the upper transition level, A_{ik} is the Einstein coefficient for the transition i, $h\nu$ is the transition energy and β is the escape probability. Katsova (1990) published an analysis of Balmer decrements of red dwarfs during flare and in the quiescent phases. This analysis is limited to electron densities of 10^{13}-$10^{14} cm^{-3}$ and electron temperatures 10000-15000 K.

Some constraints on the temperature and density structure can be obtained from line fluxes, especially from the Balmer lines, and from He and higher excitation lines. The broadening and merging of higher Balmer lines, dominated by the Stark effect, can be used to estimate electron densities in the chromosphere (Donati-Falchi et al. 1985). Measurements of the broadening of the lower Balmer lines, which are less affected by the Stark effect, together with line shifts, provide information on the large scale motions during flares.

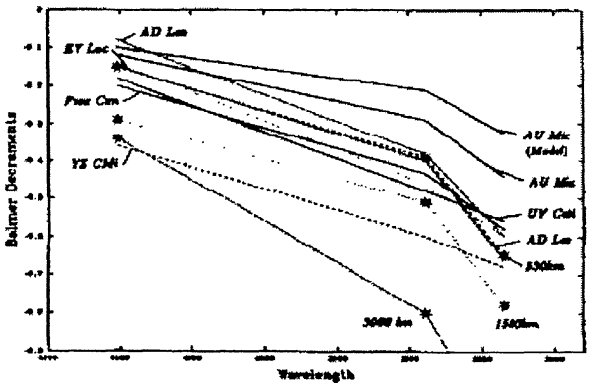

Fig. 5. Logarithm of the observed $H\delta$,$H\epsilon$ and$H\zeta$ Balmer decrements with respect to $H\gamma$ for spectrophotometric observations of M dwarfs

Fig 5 shows the $H\delta$,$H\epsilon$ and$H\zeta$ decrements with respect to $H\gamma$ for spectrophotometric observations of M dwarfs, the Sun . As we can see the most active stars, AD Leo and AU Mic, have the largest decrements. Since escape coefficients diminish with the plasma optical thickness and the spectral line opacity, this is evidence for large optical depths and densities between $10^8$and $10^{12} cm^{-3}$, while shallow Balmer decrements indicate electron densities larger than $10^{13} cm^{-3}$ in M dwarf atmospheres, increasing with the activity level and AU Mic having the densest chromosphere.

6.4. Emission Line Flare Behavior

The following features generally characterize the emission line flare behavior (Houddebine et al. 1991, Pettersen 1989).

1. HeI lines rise rapidly and follow the U-band light curve.
2. The H balmer lines tend to lag behind, $H\alpha$ is inevitably the strongest line of the series.
3. The CaII H and K lines lag still further, typically peaking 5-15 min after the flare onset.
4. The MgII lines have the slowest response, but enhancements may persist for several hours following the optical continuum flare.
5. Emission lines are often enhanced over quiescent values before the continuum flux begins to rise in the flare.
6. Emission lines reach their peak flux after the continuum peak.
7. CaII and MgII are more delayed than HI Balmer lines.
8. HeI follows the higher Balmer lines, while HeII emission is very short lived.
9. During the maximum flare emission the lines contribute negligibly to the total flare luminosity in the optical region, beginning at 5% of the U and B band fluxes near the flare peak and increasing to 20% during the tail of the flare decay.
10. Only when the continuum component has almost died out does the line flux begin to match that of the continuum - in the very late stages of the flare.

Some of this behaviors are represented in Figure 6 and Figure 7. Houdebine et al (1990) estimated a total mass loss that could affect the normal evolution of flare stars.

7. NON-RADIATIVE HEATING

It has been established that all measures of activity correlate well with one another, e.g. integrated optical flare energy, chomospheric and coronal radiative losses, rotation periods, etc. These inter-relationships contain important clues as to the nature of the global energetics of the atmospheres. Fosbury (1974) and Cram & Mullan (1979) identified the source of the Hα emission as arising in a chromosphere of increasing density as increased non-radiative heating supported higher temperatures in denser atmospheric layers. This higher density causes the Hα line to pass from radiative (Hα absortion) to electron collisional (Hα emission) control. These authors and Cram & Giampapa (1987) pointed out, however, that the presence of an appreciable Hα absortion line in the spectrum of K or M dwarfs, also required the presence of a **non-radiative** heated chromosphere, since the photospheric radiation field of such stars is not suffiently energetic to significantly populate the n=2 and higher levels of the hydrogen atom (requiring continuum photons at the wavelength of Lyα and shortward).

During the past 20 years, major advances have been made, in part due to solar and stellar observations and sophisticated

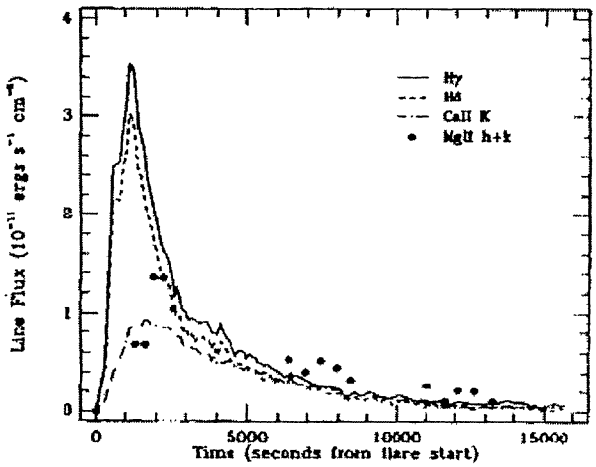

Fig. 6. The flux emitted in the emission lines $H\gamma$,$H\delta$, CaII K and MgII h&k is shown as a function of time for a flare on AD Leo

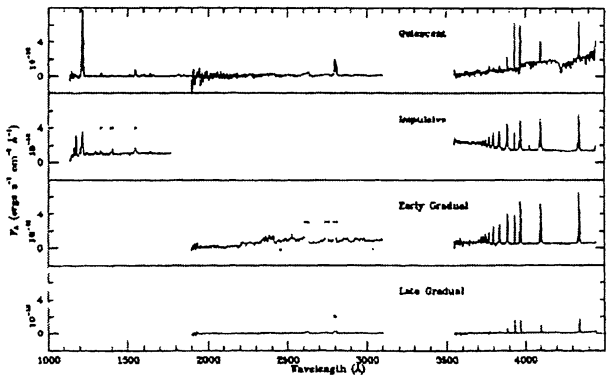

Fig. 7. Optical and ultraviolet spectra obtanied during the impulsive and gradual phases of an AD Leo flare (Hawley & Pettersen 1991)

theoretical modeling. Based on these results, it has been concluded that two different types of mechanisms for chromospheric heating exist, which can broadly be classified as **magnetic** and **acoustic** heating (see reviews by Narain & Ulmschneider 1990, 1996).

Acoustic heating depends ultimately on mechanical energy associated with convective flows. Acoustic waves, inevitably present when compressible material is forced into motion, are generated directly by convective flows, while the operation of a dynamo giving rise to magnetic fields is indirect (the field lines are stressed by the convective flows, and these stress may propogate mechanical energy to the chromosphere/corona). The acoustic source of mechanical energy is inevitably at work in all stars where convection exists. In principle, hydrodynamical codes permit one to determine the acoustic flux and spectrum in the convective zone of any star: the acoustic components of the flow are an intrinsic aspect of the same hydrodynamical equations that describe fully compressible convection itself (Hossain & Mullan 1993).

In contrast to the ubiquitous acoustic modes, magnetic modes need not be present, e.g. magnetic effects would be negligible if the stellar rotation rate is so slow that the dynamo number falls below a critical value. But even in stars where magnetic heating is at work, the atmospheric heating always includes an acoustic component as well.

7.1. Acoustic Heating

Already in the early 1950's, but particulary since the last few years it became increasingly clear that acoustic wave heating is one of the basic mechanisms which provide the mechanical energy input into the chromospheres of late-type stars. These ot outer stellar layers owe their existence to mechanical heating and would quickly dissappear (typically in a few hours), if this persistent supply of mechanical energy were in some way interruped.

For the Sun and other types of stars with surface convection zones, acoustic heating has been identified as most likely responsible for balancing the "basal" flux emission. Buchholz, Ulmschneider, & Cuntz (1998) have calculated acoustic heating models for inactive main-sequence stars and giants and have shown that the observed Mg II h&k and Ca II H&K emission can be well reproduced by those models. Similar results but for inactive M-type dwarfs have been obtained by Mullan & Cheng (1993). So far, the most sophisticated test of the acoustic heating picture has been performed by Carlsson & Stein (1992) who found that the dissipation of acoustic wave energy in the solar chromosphere can be used to reproduce the temporal variations of the Ca II K line profile observed in the solar internetwork regions. Ulmschneider et al. (1996 & 1999) showed the acoustic generation by turbulence convention.

One of the basic questions for acoustic heating is how much acoustic energy is generated in stars. One presently thinks of three ways where acoustic energy is generated in a stellar environment.

1. The simplest situation is the generation by turbulence flow fields which occur in the surface convection zones of all late-type stars. Any turbulence flow field, be it terrestrial or stellar, will invariably generate acoustic waves.
2. A second type of acoustic wave generation is the amplification of small hydrodynamic disturbances into strong wave pulses by intense radiation fields. This stochastic process is thought to be responsible for the production of strong X-ray emitting shocks in front of rapidly moving gas blobs in the winds of early-type stars.
3. A third type of acoustic wave generation in stars occurs in the magnetic regions of chromospheres and coronae where, either by mode-coupling from other magnetohydrodynamic waves, by shocks or by sudden reconnective disturbances like flares or microflares, gas pressure fluctuations are produced.

The method for the calculation of acoustic energy generated by the convection zone is based on the fact that the convective elements transfer a certain part of their kinetic energy to the ambient medium once they reach the upper boundary

of the convection zone, i.e when they slow down in the stable layer. The energy in these waves increases with the eighth power of the turbulent velocity and is also proportional to the density in the turbulent layer. The acoustic flux decreases rapidly down in cooler stars and increases rapidly as one moves to the giants and supergiant branches. For typical chromospheric conditions it has been found that the acoustic fluxes simply scale like the pressure:

$$F_m = 2.3 \times 10^4 p \quad (3)$$

The acoustic fluxes decrease rapidly and at the top of the transition region reach very small values.

7.2. Magnetic Activity

Magnetic heating is the other important mechanism for chromospheres and coronae of late-type stars (Narain & Ulmschenider 1996). Magnetic related activity is an important source of variability among stars, particulary for main sequence stars of spectral type later than G0. For stars later than K5, it may attain astonishing levels and induces important chromospheric and coronal radiative losses, rotational modulation, magnetic braking, modification to the bolometric luminosity, and possibly mass loss. Our understanding of magnetic activity is therefore crucial to that of stellar characteristics in general. In the case of the Sun, the magnetic activity is governed by the large variety of magnetic surface structures (e.g., Schrijver 1996). In various other stars, the existence of magnetic heating can directly be inferred from the observed increase of the chromospheric and transition layer emission with stellar rotation that has been found in both dwarfs (Rutten 1986, 1987; Schrijver 1987) and (sub-)giants (Rutten 1987; Rutten & Pylyser 1988; Simon & Drake 1989; Gray 1989; Strassmeier et al. 1994). Increased stellar rotation usually leads to an increased photospheric magnetic flux ($\propto B_0 f_0$), where B_0 is the photospheric magnetic field strength and f_0 is the magnetic filling factor. In fact, it is now possible to link $B_0 f_0$ to both the stellar rotation period P_{rot} (Marcy & Basri 1989; Montesinos & Jordan 1993; Saar 1996a; see also Cuntz, Ulmschneider, & Musielak 1998) and to the emergent chromospheric emission flux (Saar & Schrijver 1987; Schrijver et al. 1989; Montesinos & Jordan 1993; Saar 1996b; Jordan 1997).

Accurate measurements of stellar surface magnetic field strengths and fractional area coverages can provide empirical constrain on such important theoretical problems as the nature of dynamos, mechanism for non-radiative heating in outer atmospheres, and the evolution of stellar angular momentum and interior properties (Marcy 1984). Understanding the magnetic properties of dMe flare stars is of particular interest, due to the enormous enhancement of their activity indicators relative to those of normal solar-like stars. The greatly enhance level of this activity relative to the Sun suggets that substantial fractions of their surfaces are covered with magnetic regions (Linsky et al. 1982).

Most of the work carried out on magnetic activity in M dwarfs has, until recently, concentrated on the most active stars i.e. the dMe or Hα-emission stars. Cram & Mullan (1979) and Cram & Giampapa (1987) pointed out that the presence of Balmer absortion is indicative of the presence of a stellar chromosphere of apreciable density in the K and M dwarfs, since the photospheric radiation field alone in not enough to populate the second and higher levels of the hydrogen atom to any significant extent. Therefore significant amounts of non-radiative heating must be taking place in the atmosphere of the Balmer absortion M dwarfs. Estimates of the chromospheric radiative loss rates from these stars, based on MgII h&k and CaII H&K fluxes, lead to a similar conclusion i.e. that there exist chromosphere in the dM dwarfs but that the chromospheric heating rates are an order of magnitude or more lower than in the dMe stars (Byrne et al.,1980, Byrne et al. 1985). Although Doyle & Byrne (1986) and Doyle et al. (1986) have reported that in respect of the optical flaring, there is no fundamental difference between the dM and the dMe stars except in terms of their overall flaring energy budget. Giampapa (1985) clonchuded, from a study of chromospheric emission lines (i.e. Hα,MgII h&k and CaII H&K), that the fraction of the surfaces of the dM stars which were covered by solar plage-like regions of magnetic flux concentration was large, up to 25% for the most active dMe dwarfs. Byrne & Doyle (1989) observed weak upper-chromospheric and transition region emission from dM stars using deep UV spectroscopy, determining Lyα for the two stars for the first time, they showed that the transition from weakly active dM to active dMe star is probably due to increasing surface coverage by solar-like active regions.

7.2.1. Magnetic Dynamo

The dominant component of non-radiative heating in late-type dwarfs arises from magnetic fields which are generated in the convection zone and are transported to the surface. In stars with convective envelopes, however, the magnetic fields are generated and maintained by the self-consistent dynamo action, similar to the solar dynamo, a situation where the motion of the conducting fluid and the magnetic field induce an electric field which drives just the right current **J** to regenerate **B**.

The interaction between the magnetic and the velocity field can be described by the dynamo equation

$$\frac{\partial \mathbf{B}}{\partial t} = \nabla \times (\mathbf{v} \times \mathbf{B} + \alpha \mathbf{B}) + \eta \nabla^2 \mathbf{B} \quad (4)$$

where **B** is the magnetic field strength, t the time,**v** the velocity field,η the magnetic diffusivity and $\alpha\mathbf{B}$ term is the field caused by the fluctuating velocity field. The coefficient α, which has dimension of velocity, is a measure of the mean rotational speed of the eddies.

During the dynamo action three processes may be distinguished

1. The differential rotation which pulls the magnetic field lines in the direction of rotation and creates a strong toroidal component, w effect.
2. Poloidal fields may be regenerated from the toroidal by the cyclonic motions of the convective cells. The rate of regeneration depends on the poloidal field and a coefficient α which is a measure of the rotational speed of the eddies, α effect.
3. Turbulent diffusion is important in dynamo action since it results in the field lines being entangled with the net result that the field is spread over a larger volume.

7.2.2. Measuring Magnetic Fields

Unfortunately the lack of spatial resolution on stars together with the possible bipolar structure of magnetic regions, imposes serious problems when we try to use solar techniques for estimating stellar magnetic fields. There is a good correlation between rotation period (or better yet, Rossby number) and emission from chromospheres, transitions regions and coronae (Rutten & Schrivjer 1987). Together with observations of the solar magnetic cycle, this suggets that heating in the upper atmosphere is related in part to magnetic fields generated by a dynamo. Details of both the dynamo and heating mechanism are poorly understood, in part because stellar magnetic fields are difficult to measure. Because the Sun is a relatively inactive star, extrapoling solar results to other spectral types and/or to more active stars is speculative. At the same time, studies of stellar magnetic fields provide an important context for interpreting solar data. Johns-Krull & Valenti (1996) demonstrated a valuable technique for measuring magnetic fields on active M dwarfs.

Magnetic fields on late-type stars have typically been measured by comparing two or more line profiles that cover a range in magnetic sensitivity (Basri & Marcy 1994). Large measurement errors are common because the splitting of the Zeeman σ components in the optical is less than the intrinsic line width due to thermal, turbulent, collisional, and rotational broadening. For late-type stars, σ components have been resolved using spectral lines in the infrared, where the Zeeman effect is enhanced. On the other hand, IR spectrographs are not yet as efficient as optical spectrographs, so intrumental limitations have been made using IR diagnostics to measure stellar magnetic fields (Saar 1994, Valenti, Marcy & Basri 1995).

The field strengths on active M dwarfs are so large that the σ components are split out of the core of the FeI line at 8468.40Å. This means we can use efficient optical spectrographs to measure accurate magnetic field parameters for M dwarfs, while circumventing the difficulties currently associated with high-resolution infrared spectroscopy. Using the FeI line at 8468.40Å together with other spectral diagnostics, Johns-Krull & Valenti (1996) have begun to measure magnetic field parameters for several nearby M dwarfs.

7.2.3. Activity-Rotation-Age Connection

It is widely accepted that rotation is a fundamental parameter in determinig the activity levels (dynamo action) in late-type stellar atmospheres in the sense that, the shorter the rotation period of a star, then the higher its activity level. This appears to hold over a wide range of spectral types from F to M. Observationally, this activity manifests itself in the form of flares, spot modulation of visible light and strong emission from the non-radiatively heated chromosphere and coronae. All of these phenomena are seen in their most extreme forms in the emission line dwarf M stars. There are basically three methods for obtaining the rotational velocities.

1. The line profile is calibrated in terms of a rotational standard which is used as a template.
2. Another method uses radiative transfer techniques to calculate a line profile, broadened with rotation, taking into account macroturbulence and then comparing the model to the observed line profile. The lines chosen should be insensitive to magnetic fields, so that Zeeman splitting is not interpreted as due to rotation.
3. The third is to measure directly the period using the rotational modulation of atmospheric inhomogeneities in lines as well as white light.

There are several line of evidence for an association between fast rotation and chromospheric activity, such as an empirical rotation and emission in the Ca II H&K and MgII h&k lines (Doyle 1987). The ratio of rotation period to convective turnover time, also known as the Rossby number, is often used instead of the rotational velocity. No matter which parameter is used, the major conclusion from these relationships is that the faster rotators have the strongest emission. Also there is a very close link between activity, rotation and age, in the sense that with increasing age the rotational rate decreases and consequently the atmospheric activity. Late-type dwarfs are believed to be braked by mass loss carried by the stellar winds thereby transferring angular momentum from the star to the interstellar medium, however, not many observations of mass loss from late-type dwarfs exist to date.

7.3. Microflares and others mechanism of non-radiative heating

A large variety of non-radiative heating mechanism have been put foward over recent decades, including Alfven waves (Steinolfson & Davila 1993), current dissipation (Rosner,Tucker & Vaiana 1978), inverse bremsstrahlung (Øien & Alendal 1993) and electrodynamic coupling (Ionson 1984). One very promising mechanism was proposed by Parker (1981,1983) and involves the dissipation of magnetic energy at numerous "magnetic discontinuities" within individual flux tubes. These are thought to be formed by the random motions of the magnetic fields resulting from their interaction with the stellar convection. The energy released in each event was estimated as 10^{24} to 10^{25} ergs, about 10^{-9} of the energy released in a large solar flare. Because of this, Parker (1988) referred to them as nanoflare events. Individual events cannot be resolved, even on the Sun. However, it is thought that individual energy releases can result in a cascade within an unstable flux tube and will result in detectable microflares or normal flare events (see, e.g., Lu & Hamilton 1991; Lu et al. 1993). Support for this theory comes from the fact that both the emission measure distribution and the extreme-UV and X-ray emission-line spectra for active stars are compatible with a flare-heated plasma (e.g., Raymond 1990; Güdel 1997).

In the higher energy domain the nanoflares are normally referred to as microflares. Unfortunable not much is known about microflaring activity on others stars, although there is some evidence that stellar flaring is related to coronal heating. For example, Doyle & Butler (1985) and Skumanich (1985) independently examined the activity in dMe flare stars and discovered a linear relation between the time-average U-band flux from flares and the quiescent X-ray emission over more than 3 orders of magnitude in X-ray flux. Butler et al. (1986) also showed a correlation between soft X-ray fluctuations and small, flarelike events seen in the integrated $H\alpha$ on several active stars. This study has been questioned by Pallavicini, Tagliaferri & Stella (1990), who found no evidence for statistically significant variability on timescales less than a few minutes in a large sample of EXOSAT data.

Microflares events are small, often having fluxes at or less than the background against which they are mesaured. To detect these events it is necessary to bin the individual time sequences and then search the binned series for elements that have counts significantly higher than would be expected by chance. Strong events show up at small binning intervals, while the weaker events sometimes require binning over their entire duration before a significant number of counts are detected. To determine which events are statistically significant it is necessary to determine a probability distribution for any given binning factor.

Larger events appear to consist of closely packed groups of smaller flares, perhaps representing a cascade in which each component represents the excitation of one loop or loop arcade within an active region (Machado et al. 1988). These individual components may be more apparent in the UV than the optical because of the much shorter decay time at these wavelenghts; i.e, flares are known to be very blue initially and to redden rapidly with time (Katsova & Livshits 1991).

The data suggest that the energy distribution of nanoflares is significantly different from normal flare and microflare events, in agreement with previous authors.

To test whether microflare events are important in the heating of stellar coronae, it is necessary to measure these events down to the lowest possible energies, testing whether the occurrence rate continues along the power-law distribution known to exist for more energetic events. Such events have already been detected on the Sun (Lin et al. 1984), although there is some debate about whether their energy is sufficient to heat the solar corona (Porter, Fontenla & Simnett 1995). Unfortunately, ground-based optical monitoring of stellar flares is limited with regard to the intensities of the flare events that can be detected, both because of the seeing effects within the atmosphere and the large photospheric background against which the flares are observed. To overcome these difficulties, Robinson et al (1999) obtained near-UV photometric time sequences for two nearby M dwarf stars using the high-speed photometer (HSP) on board the Hubble Space Telescope (HST). The photospheric flux of these cool stars is negligible below 3000$\AA$, so essentially all radiation observed by the HSP will originate in the stellar chromosphere, where the effects of the microflares should be pronounced.

8. SPECTRAL LINE CONSIDERATIONS OF MODELS ON LATE-TYPE STARS

In recent years, different authors have take into account several mechanism that have an important influence on atmospheric models.

8.1. Hydrogen Recombination

The Hydrogen recombination continua is an important spectral diagnostic of stellar atmospheres. They can contribute significantly to the cooling in the outer layers such as the upper chromosphere (Balmer continuum) and the transition region (Lyman continuum). Because of their high sensitivity to electron density, they can also provide valuable constraints on the pressure and amount of plasma in their respective region of formation. Because their optical depth is smaller than those in spectral lines, they are complementary diagnostics and their penetration deep in the atmosphere can play an important role in the local ionisation equilibrium and the formation of spectral lines (Houdebine et al. 1995 for M dwarfs; Vernazza et al. 1981 for the Sun; Avrett et al. 1986 for solar flares).

8.1.1. Electron Densities

Houdebine et al. (1995) gave chromospheric electron density domains for M dwarf, K dwarfs and the Sun (Table 1), as obtained from various NLTE studies. They also communicate the associated column mass domain for the base of the transition region. Both quiescent and flaring cases were given. Those values are also plotted in Figure 8. This diagram is useful so as to visualize and intercompare these domains in the Sun and other stars. In Figure 8, one can depict the electron density rise as a function of the transition region column mass-i.e.- as a function of the transition region pressure (or activity level for M dwarfs). The range of electron density for a given atmosphere is also much larger for later type stars due to the lower minimum temperature. Even without considering radiation transfer problems, this implies that there should not be a tight one-to-one flux correlation between spectral lines formed in the upper chromosphere or transition region and others formed in the lower chromosphere. One can also notice that the domains for high activity M dwarfs and the solar flares are quite similar, even though the column mass range is different. This again emphasizes the low ionization fraction of hydrogen in M dwarfs chromospheres.

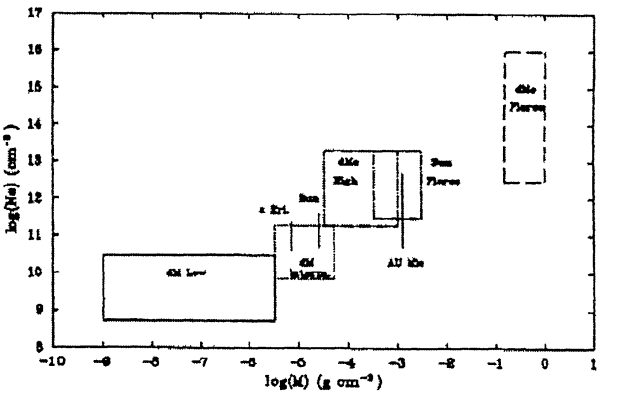

Fig. 8. Electron density regimes in the chromosphere versus the transition region column density for M,K and G main sequence stars from NLTE-radiation transfer calculations (Houdebine et al. 1995)

8.2. Line Blanketing

Due to the presence of numerous spectral lines on dM stars, both atomic and molecular, it is very important to include in the opacity calculations the contribution of this bound-bound absorption, generally referred to as line blanketing (Andretta et al., 1997, Short & Doyle, 1997).

An assumption usually made to simplify the modelling process, is to consider that all the minority species not explicitly considered for the emergent line spectrum, are in Local Ther-

Atmosphere Type	N_e (cm^{-3})	log(M) (g cm^{-2})
M dwarf Low Activity	[5 10^{8} : 3 10^{10}]	< −5.5
M dwarf Intermediate Activity	[7 10^{9} : 2 10^{11}]	[−5.5 : −4.3]
M dwarf High Activity	[2 10^{11} : 2 10^{13}]	[−4.5 : −3.0]
M dwarf Flare Kernels	[3 10^{12} : 10^{15}]	[−0.8 : 0.0]
K2 dwarf ϵ Eridani	[5 10^{10} : 4 10^{11}]	−4.54
Sun Quiescent	[4 10^{10} : 2 10^{11}]	−5.15
Sun Flare	[3 10^{11} : 2 10^{13}]	[−3.5 : −2.5]

Fig. 9. Chromospheric electron density for M dwarfs stars and the Sun (Houdebine et al. 1995)

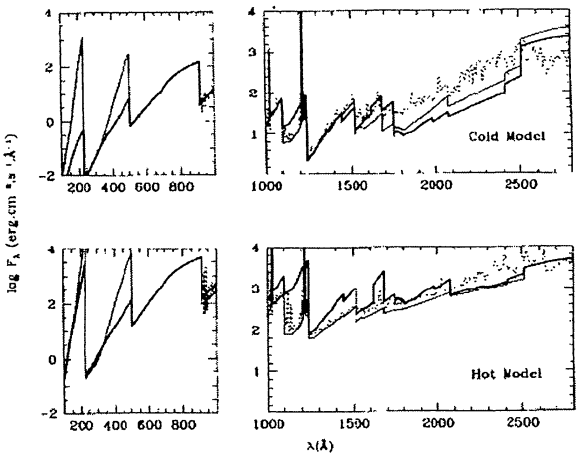

Fig. 10. Continuum flux computed for cold model (upper panels) and hot model (lower panels). The "cold" chromospheric model corresponds to a low activity dM star and the "hot" one to a very active dMe star. Thick line: metals in NLTE, without line blanketing. Thin line: metals in LTE, without line blanketing. Dotted line:metals in LTE, with line blanketing (Falchi & Mauas 1998).

modynamic Equilibrium (LTE), i.e., that their level populations are described by the Saha and Boltzmann equations.

In other words, if only the continuum and/or the hydrogen lines are used as spectral diagnostics, the only species computed outside LTE is hydrogen. If some other spectral line is also considered, then this species is computed outside of LTE and the others are still assumed in LTE.

Most of the chromospheric models computed up to now, neglected the line blanketing due to the numerous atomic and molecular lines present in the stellar atmosphere. However, we have already pointed out that, for active stars, the continuum levels computed with and without line blanketing are very different and therefore result in very different values for the colors of the star.

Only recently, Andretta et al. (1997) included line blanketing at photospheric levels, and Short & Doyle (1997) included it also at chromospheric levels and examined the dependence of computed line profiles on background opacities.

To neglect line blanketing when computing the background opacities, affects strongly not only the computed continuum, as expected, but also affects the population balance between different levels of the atomic species under consideration, and therefore the computed line-centre intensities (Figure 10).

8.3. Dust

Jones & Tsuji (1997) draw attention to the 0.65-0.75 μm region of the spectra of late-type M dwarfs, where they found that the TiO molecular absorption bonds decrease rather than increase in strength toward later spectral types. This decrease is not expected from synthetic spectra unless the effects of dust formation are included. They made a comparison between M dwarf spectra and the predictions for dusty and nondusty models (Figure 11). They focus on the region shortward of 1 μm where the effects of dust formation are largest and can clearly be distinguished from the problems with reliable modeling of water-vapor absorption bands. The implication of their work is that dust needs to be considered in models of objects below 3000 K. This is necessary to enable a better fit with observed spectra and photometry, for the derivation of evolutionary tracks for objects below 3000 K, and to find a reliable value for the hydrogen-burning limit. In addition they caution against the use of specific molecular bands for assigning spectral types in late-type M stars.

9. MODELS OF STELLAR-SOLAR ATMOSPHERES

Despite recent progress in imaging techniques, the structure of surface inhomogeneities in the atmospheres of late-type stars remains largely uncertain, especially at layers above the photosphere where spectroscopic lines are formed in NLTE. Furthermore, at least in the more active stars, one may expect that turbulence and mass circulation, similar to that observed in the solar atmosphere, play an important role in the energy transport and therefore in the atmospheric morphology. However, a physical description of these is still very approximate.

One dimensional models provide some kind of average information about the atmosphere. However, since the averaging process is non-linear, such models can provide only a rough indication of the physical conditions of the atmosphere and they could fail, for instance, in reproducing spectroscopic signatures

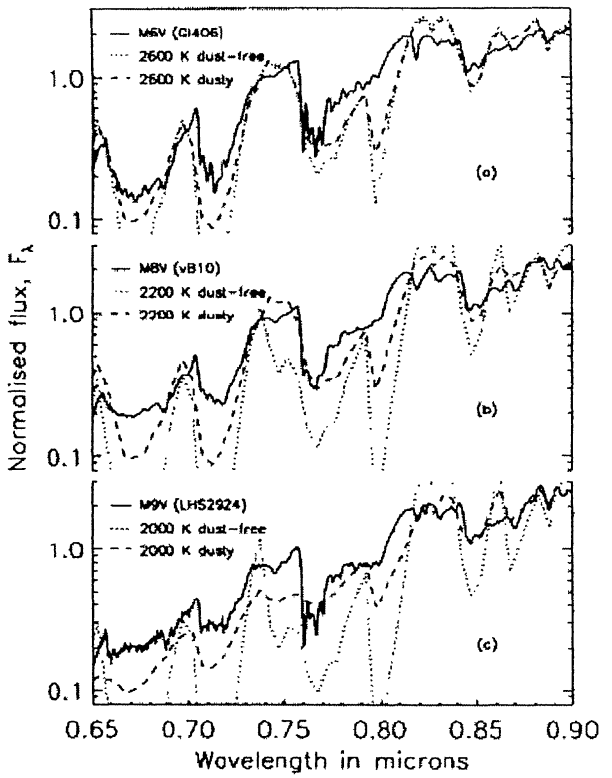

Fig. 11. Comparison between observed spectra (solid curves), dusty models (dashed curves) and dust-free models (dotted curves) (Jones & Tsuji 1997)

formed in overlapping regions (Giampapa, Worden & Linsky 1982).

The assumption of one dimensional geometry in the calculation of particle transport, including radiative transfer, is justified when the characteristic length of variation of all the relevant parameters in a particular direction (the direction of the stratification) is much smaller than that in the perpendicular direction. This may occur for cases in which the vertical stratification occurs over short distances compared with the horizontal variations. Although this might be considered a crude approximation, it nevertheless gives the possibility of studying many important physical processes which would otherwise remain unexplored.

The chromosphere is generally defined as the part of the solar or stellar atmosphere beginning in the temperature minimum region above the visible surface, and extending upward to the altitude where a very steep temperature gradient forms a transition zone separating the chromosphere and the corona. This definition implies that the atmosphere is thermally stratified in horizontal layers. Such a one dimensional description is of limited validity at best. Yet it does provide a useful framework for understanding many aspects of the chromospheric physics, as long as we recognise that in the real dynamic chromosphere, the temperature, density, magnetic field, and velocity all vary in three dimensions and time.

From observational evidence and by analogy with the Sun, we know that in the atmosphere of late-type stars the chromosphere and the transition region are horizontally inhomogeneous and these inhomogeneities are pervasive and mostly short lived. In the stellar case, where virtually no spatial information is avaliable, the atmosphere should be ideally described in terms of distribution functions for the thermodynamic and magneto-fluid-dynamic variables. A determination of the state of variables may derive from spectroscopic diagnostics, i.e., from the observations of spectroscopic signatures associated with theoretical techniques to infer thermodynamic or magneto-fluid-dynamic quantities. Especially when applied to the red dwarf case, this process faces many difficulties, among which are the paucity and inaccuracy of the spectroscopic observations, the complexity of the observed spectra and the modelling of the formation of optically thick spectroscopic lines. Therefore, obtaining meaningful average values of the state of variables and mean model atmospheres has proven to be difficult.

A model of a stellar atmosphere, in its simplest form, is described by a T(height), T(m) or T(τ) relation. Height is defined as distance above some reference point and m is the column mass above the point defined as:

$$m = \int_{\infty}^{z} \rho(z) dz \tag{5}$$

where ρ is the density of the material and τ is the optical depth as defined by:

$$d\tau = \kappa \rho dz. \tag{6}$$

Such models can be used to interpret the temporal and spatially averaged radiative energy that is recorded in stellar spectra. The following assumptions normally apply:

- the ideal gas law ($P_g V = n_{mole} RT$)
- the Maxwell distribution
- time-independent equilibrium (statistical equilibrium or local thermodynamical equilibrium)
- 1-D stratification (no spots or other inhomogeneities)
- hydrostatic equilibrium (no waves, accelerations, mass loss)

9.1. Modelling Approaches

In the recent literature there exist several different approaches to the modelling of stellar atmospheres.

1. **Radiative Equilibrium.** The atmospheric structure is determined so that the net radiative flux is constant with depth. The effects of convective energy transport are also often included, in the deeper layers. Models assuming radiative equilibrium do not reproduce the outward increase in temperature inferred from stellar chromospheric observations (Avrett 1996). Therefore such models are completely inadequate for modelling the stellar atmosphere of an active star with a chromosphere and even less for a flare atmosphere.
2. **Semi-empirical modelling.** For "semiempirical" we mean that, given a T vs. z distribution, we self-consistently compute non-LTE populations for H, He, Fe, Si, Al, Ca, Na and Mg, solving simultaneously the equations of hydrostatic equilibrium, radiative transfer, and statistical equilibrium. The temperature distribution in the atmosphere

is chosen by a trial and error approach to obtain a good agreement between the calculated and observed spectra. This procedure replaces the constant net radiative flux constraint in determining the temperature distribution with height. The radiative cooling rate (derivative of the radiative flux) gives the distribution of mechanical heating that would be needed to produce the given temperature distribution. Such semi-empirical models are strongly dependent on the type of solution of the radiative transfer problem used. For the semi-empirical modelling of stellar chromospheres and stellar flare atmospheres it is necessary to use non-LTE radiative transfer. Departures from local thermodynamic equilibrium in the populations of the levels of the most important elements for radiative losses such as Hydrogen, singly ionized Magnesium and singly ionized Calcium can be huge. This leads to an inadequate estimate of the cooling and heating in the atmosphere. To model a stellar flare atmosphere one can use two different approaches: either an *ad hoc* approach, to add a hot region at some level of the quiescent atmosphere, then solve coupled equations of radiative transfer and hydrostatic equilibrium (e.g. Houdebine 1992) or to try to develop a model by fitting emission lines assuming that the flare occurs only in a limited region of the stellar surface (e.g. Mauas and Falchi 1996).

In the one dimensional, hydrostatic approximation, semi-empirical chromospheric models for late-type stars have been usually inferred by

(a) Choosing a model photosphere which is appropiate for the given spectral type and luminosity.
(b) Postulating a temperature distribution for the chromosphere which is put on top of the photospheric model.
(c) Solving the NLTE radiative transfer problem for the given temperature structure and atomic model considered.
(d) Systematically adjusting the chromospheric temperature distribution to achieve the closest possible agreement between theory and observation.

3. **Hydrodynamical (gas-dynamical) modelling**. One can solve time-dependent equations for mass, momentum and energy conservation. Hydrodynamic loop models of flares aim at calculating the evolution of confined plasma during the thermal phase of flares, under simplifying hypotheses. They achieve a reasonable level of detail and of realism by describing the simultaneous influence of the effects dominating the thermal phase of flares (thermal conduction, compresible hydrodynamics, radiative losses), in the fully non-linear regime and in the loop-like geometry shown by observations. Hydrodynamic models of flares can provide a link between the well-observed thermal phase and the primary effects. After the model has provided a satisfactory reproduction of the observations, one can impose constraints on the primary mechanism using the parameters of the model yielding the best agreement. For instance the localization and extension of the heating function used in the model, as well as the timing required to fit a flare. Analogously the computed maximum plasma pressure provides a lower limit on the magnetic field needed to confine the plasma. Of course some diagnostic power lies also in the possibility of proving the ineffectiveness of some specific mechanisms. This approach exposes the diagnostic possibilities of hydrodynamic models, an interesting expansion of their use as theoretical tools.

9.2. Codes

There exist several different popular radiative transfer codes often used in modelling stellar (solar) atmospheres although some authors use their own codes.

1. **Pandora** is a general-purpose non-LTE computer program for calculating stellar atmospheric models and spectra. This code solves the multi-atom, multi-level statistical equilibrium equation together with the radiative transfer equation using either partial or complete frequency redistribution in plane parallel or spherical geometry (Avrett & Loeser 1992).
2. **MULTI** (Carlsson 1986) is a program for solving multi-level non-LTE radiative transfer problems in semi-infinite, plane parallel one-dimensional atmospheres with a prescribed macroscopic velocity field. The lines are assumed to be formed with complete redistribution over the profile function which is assumed to be a Voigt function. A partial redistribution upgrade of this code (Uitenbroek 1989) exists with extension to spherical geometry Harper (1994). The MULTI code is very well documented and allows the user to introduce changes which are very important for modelling atmospheres of late type stars (introduction of molecular and line opacities).
3. **PHOENIX** is capable of solving the radiative transfer equation in the Lagrangian frame self-consistently with multilevel, non-LTE rate equation in the Lagrangian frame. Numerical methods used in PHOENIX include the solution of:
   (a) The radiative transfer equation using the accelerated lambda iteration (ALI) method described by Hauschildt (1992)
   (b) The multilevel non-LTE continuum and line transfer prblem using the ALI alogorithm (Hauschildt 1993)

   Important additions to PHOENIX were necessary to handle the problems specific to compact dwarf atmospheres (Allard & Hauschildt 1995). Additional changes are currently ongoing at Armagh Observatory.

9.3. A Two-ribbon Flare Model

Several flare scenarios have been developed. The difficulty is to explain the trigger mechanism, the timing of the various flare components (radiation, ejecta, and accelerated particles) and the changing spectral distribution over a huge range of wavelengths as the flare evolves. No model has been able to describe all aspects, nor do we have a reliable and comprehensive energy budget (Haisch et al. 1991).

Kiepenheuer (1964) first proposed that two-ribbon flares and filament eruptions are different manifestation of the same phenomenon, and some researchers have concluded that all flares are driven by eruptions (Moore 1988, Zirin 1988). A concept for the magnetic configuration and location of the major physical phenomena was first presented by Carmichael (1964).

Figure 12 illustrates most aspects of this scenario with a cross section perpendicular to the photospheric polarity inversion line. The lines with arrows are the magnetic field **B** projections. Owing to the presence of a magnetic field component perpendicular to the figure, the closed field lines represent a helical flux tube that connects back to the photosphere at the

endpoints of the filament. So contrary to appearance, there are no open field lines. The existence of closed (in projection) field lines implies the presence of a net current in the direction of the axis of the filament (the centre of the tube). This current is the ultimate source of free magnetic energy that fuels the flare.

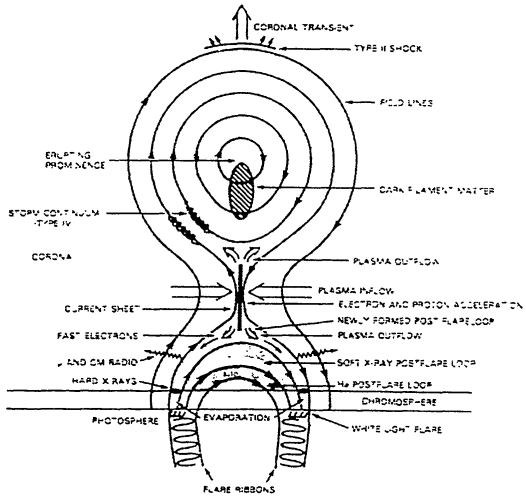

Fig. 12. The global structure of the Martens & Kuin two-ribbon flare model showing the location of the major observed energy conversion processes, viewed in a cross section along the neutral line (Martens & Kuin 1989)

Prior to the two-ribbon flare, the filament erupts. The eruption may be caused by:

a) "loss of equilibrium" as the filament current surpasses a certain threshold (Low 1977);
b) a slow withering away of the overlying arcade of coronal loops by gentle preflare reconnection in the current sheet below the filament (Sturrock et al. 1984), until, again loss of equilibrium sets in;
c) a different scenario - supported by the numerical MHD model of van Ballegooijen and Martens (1989)- in which the equilibrium height of the filament increases at an accelerating rate in response to photospheric magnetic flux cancellation. In this scenario, loss of equilibrium never occurs, but an eruption is still initiated.

As the filament erupts the reconnection rate in the current sheet in its wake is strongly enhanced because of field gradients created by stretching of the whole field configuration. The energy released by the reconnection in this sheet fuels most of the two-ribbon flare phenomena.

Two types of theories have been proposed to explain how the flare energy, which is released in the upper corona by magnetic field reconnection, is transported down to the lower layers which emit optical and UV radiation (chromosphere, photosphere). These theories assume either beams of energetic particles (electrons, protons) or thermal conduction. Different predictions come from these theories. Depending on the penetration length, electrons of a given energy can reach the chromosphere, transporting significant energy and producing a detectable signature, for example in the Balmer wings. If the electrons are stopped in the corona, thermal conduction is then required to transport most of the energy downwards. These analyses have been refined in order to take into account non-classical Coulomb effects and the role of currents and wave-particle interaction (Foing, 1989). Emslie & Nagai (1985) predict a different temporal evolution of transition region lines by the two mechanisms, which can be checked observationally using far UV and extreme UV spectroscopy.

9.4. Chromospheric Models

The first attempts to model the chromospheres of dM stars where those by Cram & Mullan (1979), who assumed very schematic chromospheric models and studied the response of the emitted Balmer lines to changes of different atmospheric parameters. They found that, as the temperature gradient in the chromosphere increases, the very weak H_α line predicted for a star with an isothermal chromosphere first becomes an increasingly strong absorption line, then gradually fills in and eventually goes into emission as the chromospheric temperature increases further.

Giampapa et al. (1982) constructed homogeneous models in a similar way, to explain the profiles of the Ca II K line for some representative dMe and dM stars. They found that their models did not predict the right flux for the Mg II resonance lines, and concluded that the assumption of a homogeneous chromosphere was unrealistic.

Houdebine & Doyle (1994a), and Doyle et al. (1994) recently presented grids of atmospheric models, which were merged in Houdebine et al. (1995). They studied the influence of the atmospheric structure on the hydrogen and Ca II line profiles. Houdebine and Doyle (1994b) applied this modelling to the dM2.5e star AU Mic. They obtained very good agreement with the observed profiles for H_α and H_β, but they had to add an arbitrary constant to their computed profiles, in order to match them with the observations. In their model, the position of the transition region is fixed to obtain a ratio between the H_α and the Ly_α flux of about 1.1, as was found by Doyle et al. (1990). However, they treated Ly_α assuming Complete Redistribution, which has been shown to be a rather poor approximation (e.g. Vernazza et al. 1981).

Hawley & Fisher (1992) computed a theoretical model of the quiescent atmosphere of AD Leo (Gl 388) from the photosphere to the corona. The structure of the corona and the transition region is computed for a loop of length $L = 10^{10}$ cm and an apex coronal temperature of 3 10^6 K, in hydrostatic and thermal equilibrium. The photosphere is taken from the grid of models by Mould (1976). The chromosphere is a linear log T - log m interpolation (where m is the column mass) joining the transition region and the photosphere. They use this model only to determine the quiescent heating rate necessary for the computation of flare models and their results do not fit very well the observed spectral features of the quiet star.

Mauas & Falchi 1994 presented a semiempirical model for the dM3.5e star AD Leo, computed to match a wide set of observations. They obtained very good agreement for the continuum level, the first four Balmer lines, the Na D and infrared lines and the Mg II flux. However, the agreement was not so good for the Ca II K line profile, and for the Ly_α flux, for

which they found a difference between the observed and computed features of about a factor of two. The resulting model was used in Mauas & Falchi 1996a as the base for modelling a large flare on the same star. They believe the approach of semi-empirical modelling, where an atmospheric model is constructed to find the best possible agreement between the computed profiles and a large number of observations, is the one that gives the best results to eliminate the uncertainties found when only a few lines (generally H_α or Ca II K) are matched.

Mauas & Falchi 1997 presented chromospheric models for two M dwarf stars considered as "basal" stars due to the very low level of chromospheric activity, to be compared with the model for a very active, flare star, AD Leo. These models are not based on a single spectral feature, but on many lines corresponding to three different atoms, the continuum in a broad wavelength range, from the ultraviolet to the infrared, and the Mg II h and k flux. All in all, the agreement between models and observations is remarkably good. Comparing the dM and the dMe stars, they saw that, as expected, the presence of the Balmer lines in emission (and the much larger Ca II and Mg II fluxes) is determined by the structure of the chromosphere, much hotter for AD Leo than for the other two stars. This, in turn, implies a much larger electron density, and a closer coupling of the source function with the Planck function. In fact, the model for AD Leo is 2000 K hotter than the ones for the dM stars, at log(m)=-4.

From an energetic point of view, it can be seen comparing the results in Mauas & Falchi (1994) and Mauas & Falchi (1997) that the additional energy required to transform a dM star into an active star is needed in the high chromosphere, just below the transition region. The mid-chromosphere, in turn, is automatically heated by the energy emitted above it, and reabsorbed in this region, in particular, in the Mg II and Balmer lines.

Falchi & Mauas (1998) studied how different approximations, usually made to simplify the computation of chromospheric models, can affect the computed spectrum emitted by two atmospheric models: a cold one, corresponding to the low-activity dM star Gl 588, and a hot one, corresponding to the very active star AD Leo. They found that assuming that the minority species are in LTE leads to an underestimate in the electron density in the low chromosphere. On the other hand, they showed this assumption does not affect the profile of the hydrogen lines, or those of Ca II K and Na D. They concluded that if only these profiles are to be used as a modelling tool, there is no need to compute self-consistently the NLTE population of the metals. To neglect line blanketing when computing the background opacities, affects strongly not only the computed continuum, as they expected, but also affects the population balance between different levels of the atomic species under consideration, and the computed line-centre intensities. The continuum intensity effect is often neglected and the line profiles, relative to the continuum, are studied; they showed that it is not enough, since also in this case the computed profiles are very different.

9.5. Flare Models

Cram & Woods (1982) constructed a grid of models of the flaring chromosphere and the transition region of a dM2 star. They define temperature distributions which schematically represent the various mechanisms that can transport the energy from the corona. In this way they study the response of certain spectral signatures of stellar flares (Balmer lines and continuum) to these different processes. They found that the observed spectral characteristics may be explained by models with increased pressure and temperature in the flaring chromosphere. Since this might result from different physical processes they were not able to link directly a given spectroscopic feature to any particular energy transport process.

Fisher & Hawley (1990) developed a simple algorithm to calculate the response of a coronal loop to the release of flare energy over a rather long time scale. This calculation is not a complete hydrodynamical one because the authors neglect the momentum equation (time scales greater than the loop sound transit times). They also assumed that the flare heating rate is uniform in the loop and the flare loop will at any given time be in one of three proposed regimes.

Mauas et al. (1990) computed semi-empirical model atmospheres for the solar flare of 1982 June 15. They used Avrett's Pandora code and took into account nine different species (HI HeI-II, Si I, MgI-II, CI, FeI, AlI NaI, CaI-II) for which they calculated how the populations depart from LTE. They show that the flare-related perturbation affects material at photospheric depths and that it is in the photosphere, and not in the chromosphere, where the continuum emission originates.

Cheng & Pallavicini (1991) followed the procedure of Cheng et al. (1983) and Doschek et al. (1983) to make a series of numerical simulations of flare loop models with different values of loop size, flare energy input and initial loop conditions. They obtained the evolution of the flare loop parameters by solving the full set of time dependent two-fluid equations of mass momentum and energy conservation and tried to interpret observations of a large variety of stellar X-ray flares. It would be interesting to use their approach in the explanation of optical data e.g. to connect this approach with radiative transfer codes.

Katsova et al. (1991) applied a gas-dynamic model to spectra of a flare on YZ CMi, found a flare area of 5×10^{17}cm^2 and calculated Balmer decrements for the same flare. They found that the observational data agree well with the theoretical Balmer decrements for a temperature T=10^4K, electron density n_e=10^{14}cm^{-3} and an optical depth of the layer at the Lα line centre τ(Lα)= 2×10^6. Their calculations are limited to tabulated sources of optical depth of Lα and this approach should include more accurate radiative transfer calculations.

Houdebine (1992) built a grid of atmospheric models for flares in dM stars, to study the effect of different model parameters on the emerging Hydrogen and Calcium visible spectra. He used Carlsson's NLTE radiative transfer code MULTI, complete frequency redistribution, 4 angles of radiation transfer, atomic models with 15 levels + continuum for Hydrogen and 14 levels + continuum for Calcium and photospheric models by Mould (1976). The most important parameter of these models is the column mass of the transition region, assumed to be between log m=-0.7 and log m=0. These models are intended to represent very dense flare kernels, with electron densities of a few times 10^{16}cm^{-3}, as deduced from Balmer line broadening observed in some flares. The spectra computed with these models reproduce many of the observed general characteristics such as intense white light emission, the very broad Balmer lines and inverse Balmer decrement for H_α and H_β. An important point is that Houdebine used a very old photospheric

model for AD Leo and today there exist much better models which include more molecular and line opacities (Allard and Hauschildt 1995).

Hawley & Fisher (1992) computed a sequence of five models of a flaring stellar atmosphere using MULTI. They computed the response of the gas in a magnetic loop to the soft X-ray radiation emitted by the corona at a given temperature, in hydrostatic and energetic equilibrium. The effects of enhanced thermal conduction and pressure from the flaring corona are included in a self-consistent way, and cooling by radiative losses is computed in detail. Their models were constructed to investigate whether the chromospheric emission during the gradual phase can be due to X-ray heating alone. Comparison with the observations during a giant flare of AD Leo (Hawley & Petersen 1991), shows that a single model cannot fit all the observed line ratios during a certain phase of the flare. While their hottest model with a coronal temperature T=20 $\times$ 10^6 K explains the observed emission measures for lines formed in the transition region, additional heating in the upper chromosphere is necessary to explain the observed emission in the Balmer and CaII K lines. Furthermore, none of their models can explain the blue colour of the observed continuum spectrum.

Hawley & Fisher (1994) developed solar flare model atmospheres under the assumption of energetic equilibrium in the chromosphere. This model uses a static one-dimensional plane parallel geometry and is designed within a physically self-consistent coronal loop. They used very simplified atomic models (6-level plus continuum for Hydrogen, 5 levels plus continuum for Ca II and 3-level plus continuum for MgII) so their results may not be very accurate and their discussion of the formation of the H_α should be checked using more accurate atomic models.

Mauas & Falchi (1994, 1996) presented models for the quiescent and flare atmosphere of AD Leo. They used Avrett's Pandora code and calculated semi-empirical atmospheres for two different moments (914s and 1222s after flare onset).

Jevremovic et al. (1998) developed a new code for the analysis of the atmospheric response to heating during stellar flares. Their code uses a grid of 150 points and re-meshing is accomplished using changes in temperature as the control function. Their code is coupled with the radiative transfer code MULTI, which provides regular updates of the radiative losses for H, Ca and Mg. The introduction of full radiative transfer allows them to follow the spectral features during the course of the flare. This new code shows that is possible to simulate the main features occuring during the stellar flare using their simplified model. They applied their model to high temporal (aprox. 3sec) and medium resolution spectrophotometric observations of a flare on AD Leo.

Abbet & Hawley (1999) use the code of Carlsson & Stein (1997) to model the radiative-hydrodynamic response of the lower atmosphere at the footpoint of a magnetically confined flare loop. The plane-parallel model atmospheres include the upper transition region and corona in order to calculate self-consistently the flare heating due to an influx of nonthermal electrons and the soft X-ray photoionization from high-temperature regions of the atmosphere. A circular loop geometry is taken into account when calculating the X-ray photoionization rates, and a corresponding geometric correction is applied when calculating the gravitational acceleration in the upper atmosphere; otherwise the loop is treated as a vertical cylinder with homogeneous, plane-parallel layers. The heating processes in the lower atmosphere includes nonthermal heating by accelerated electrons and thermal soft X-ray irradiation from the flare-heated transition region and corona. Important transitions of hydrogen, helium, and singly ionized calcium and magnesium are treated in non-LTE. Their principal results of the analysis are the following:

1. An impulsive event can be described as having two distinct dynamic phases, each with a definite observational signature: an initial gentle phase, characterized by an atmospheric state of near-equilibrium, and a subsequent explosive phase, characterized by large material flows and strong hydrodynamic waves and shocks. The amount of time the atmosphere remains in the gentle phase is determined by the level of nonthermal heating. Excess line emission produced during the gentle phase is not significantly Doppler-shifted, and the profiles remain symmetric about their nominal line-center frequencies. Emission profiles generated during the explosive phase can be highly Doppler-shifted and distorted, reflecting the material motion and steep velocity gradients present at their depths of formation.
2. Hydrogen recombination radiation, from a high-temperature plateau formed during the gentle phase and from a chromospheric condensation formed during the explosive phase, is the primary cause of the white-light continuum brightening produced in the simulations.
3. A time lag is found between the brightening of the Paschen continuum and the brightening of the near wings of $H\alpha$, in the sense that the line wings brighten immediately, but the continuum first undergoes a slight dimming, followed eventually by a brightening. The continuum behavior is controlled by the trade-off between increased photoionization from enhanced populations of the excited states of hydrogen and increased electron density, which promotes recombination.
4. During the impulsive phase, when the accelerated electrons are directly heating the upper chromosphere, the contribution of the thermal soft X-rays to the overall energy balance in the lower atmosphere is negligible.

Jevremovic (1999) developed a new tool for analyzing the Balmer decrements during the flares and calculated the four main parameters for flare maxima: the electron density, the electron temperature, the temperature of the background source and the optical thickness of the Lyman α line. From this he calculated effective areas and compared them with the stellar surface area. The stellar surface coverage for the flares examined lies between 1 and 13%. There is no obvious dependence of the calculated parameters on the U magnitude of the flare. He introduced a new treatment of the Stark effect for the Balmer and Lyman lines into the radiative transfer code MULTI. Using this improved code he calculated model atmospheres for the two stars AD Leo and Gl 866. Quiescent models for both stars are in good agreement with observations. Simple schematic models are however not very good in representing the flaring atmospheres.

9.6. MHD Models

Theoretical models of the long-term time evolution of dynamo action are given by Schrijver & Pols (1993), Rosner et

al. (1995), Keppens, MacGregor & Charbonneau (1995), and Charbonneau, Schrijver & MacGregor (1997). The latter two studies contain a detailed MHD description of the time development of the internal angular momentum redistribution allowing estimates about the surface magnetic field strength and rotational velocities of main-sequence stars. These studies now provide the theoretical basis for explaining why the decrease of stellar rotation also invokes reduced values of $B_0 f_0$. If magnetic activity is concentrated within distinct active regions, and the star is not seen pole-on, rotationally modulated chromospheric emission will result (e.g., Baliunas et al. 1983, 1995; Char et al. 1993; Walter 1996). Chromospheric heating in magnetically active stars thus depends on B_0, f_0 and details of the photospheric magnetic field structure.

In new theoretical chromospheric models, serious efforts have been made to accomplish three distinctly different steps in the modeling process, namely, to calculate the acoustic and magnetic energy generation in the stellar convection zone, to model the propagation and dissipation of acoustic and magnetic energy at different atmospheric heights, and to simulate the formation of specific chromospheric emission lines that are then compared with observations. In all these steps, the two-component structure of stellar photospheres and chromospheres is fully taken into account. Computation of the propagation of nonlinear and radiatively damped longitudinal tube waves in the magnetically heated component is shown by several authors (Herbold et al. 1985; Rammacher & Ulmschneider 1989; Ulmschneider Zhringer, & Musielak 1991). Rammacher & Ulmschneider studied the formation of Ca II and Mg II emission lines inside magnetic tube waves embedded in the solar atmosphere for different wave energy fluxes and filling factors. Other results concerning the propagation and dissipation of longitudinal tube waves are described in Roberts (1991) and more recently by Bnte, Steiner & Pizzo (1993), Steiner et al. (1996), Fawzy, Ulmschneider & Cuntz (1998), and Cuntz, Ulmschneider & Musielak (1998).

In the meantime, progress has also been made in our theoretical understanding of atmospheric heating based on magnetohydrodynamic (MHD) waves. Herbold et al. (1985) investigated the behavior of nonlinear, radiatively damped longitudinal flux-tube waves in the solar atmosphere. They found significant chromospheric heating inside the tubes that depended largely on the wave period and the shape of the tubes themselves. They considered tube models with constant, semilinear, and exponential cross spreadings. In a subsequent paper, Rammacher & Ulmschneider (1989) also treated the formation of Ca II and Mg II emission lines for waves of different energies for cases of quiet and active solar regions with different magnetic filling factors. More recent results for the case of the Sun have been given by Steiner & Pizzo (1989), Bünte, Steiner & Pizzo (1993), and Steiner et al. (1996), who also considered two-dimensional effects. Improved models of magnetic wave energy generation have recently also become available. Ulmschneider & Musielak (1998) calculated the amount of energy carried by longitudinal tube waves as a result of the nonlinear and time-dependent response of thin magnetic flux tubes to strong external pressure fluctuations caused by turbulent motions.

9.7. Comparing Models

To facilitate the comparasion between various model atmospheres, Houdebine & Doyle (1994) plotted differents models (Figure 13). The model chromospheres for the quiet sun (Vernazza et al. 1981, Model C), solar flares (Machado & Linsky 1975, models F1 and F2), a dK5e stellar plage for EQ Vir (Giampapa et al. 1982), their AT Mic plage model and a stellar flare kernel atmosphere (Houdebine 1992 model (1)). These models cover five order of magnitudes in pressure and electron density, from the $\sim 10^{11} cm^{-3}$ for the quiescent Sun to $\sim 10^{16} cm^{-3}$ in a stellar flare Kernel. Emission in the Balmer lines occurs typically for densities above $\sim 10^{12} cm^{-3}$ in the upper chromosphere.

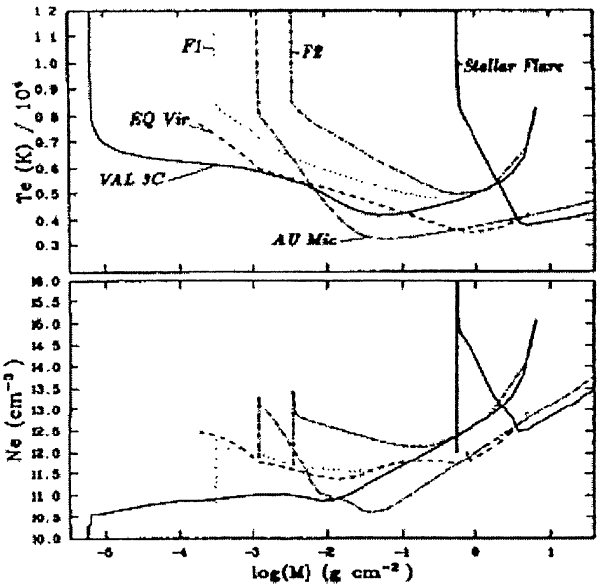

Fig. 13. Models atmospheres for the quiet Sun, solar flares,dK5e stellar plage,AU Mic plage model and a stellar flare kernel atmosphere (Houdebine & Doyle 1994)

9.8. Effects of Varying Atomic Parameters of Models

The dMe stars are a subset of the dwarf M stars which display emission in the Balmer and the CaII H and K lines, whose shapes and fluxes are evidence of a chromosphere. The fit of theoretical line profiles to observations provides valuable information on the physical processes underlying their formation as well as a detailed structure of the chromosphere. Computation of the Hydrogen lines has usually assumed radiative detailed balance in the Lyman lines or in *Lyα* (Kelch et al. 1979; Cram & Mullan 1979; Cram & Tod Woods 1982; Giampapa et al. 1982, Cram & Mullan 1985 and Cram & Giampapa 1987), and generally a 5-level plus continuum representation of the atom.

Houdebine & Panagi (1990) have studied numerically the effects of varying different atomic parameters in the NLTE modelling of Hydrogen emission lines in dMe chromosphere. They found that the most critical assumptions are the num-

ber of bound levels and the collisional data, and that the most affected lines are those between the upper levels. The Balmer decrement also changes, because variations in the atomic equilibrium are non-uniform. Furthermore, the changes in electron density may affect the computation of collisionally dominated lines such as CaII H and K. The study of detailed balance in the Lyman lines shows that, although it is a good approximation when computing Balmer line profiles, it leads to large differences in the higher Lyman members, Lyman continuum and other higher series members. They concluded that a 16 level Hydrogen atom with all line and continuum transitions between the first 5 levels provides numerical computations with enough accuracy to investigate the chromosphere of these stars.

10. PERSPECTIVES

Most of the phenomena considered to be involved in the primary cause of the flares, like magnetic field dissipation, MHD instabilities, electron acceleration etc, have been the subject of a considerable amount of theoretical work. However, directly relevant data is sparse. Most of the secondary effects, like plasma motion, hard X-rays, soft X-ray light curves and line profiles, are just a consequence of the primary effects; yet they have been observed with much higher level of detail. It will be very interesting try to improve the stellar atmosphere models taking into account MHD.

The upcoming high spectral resolution observations of the X-ray emission from both the quiescent and flaring emission from flare stars, to be performed with the Chandra and XMM observatories will allow direct measurements of the plasma pressure for a range of temperatures using selected spectral diagnostics, and thus to test the correctness of the framework presented in the present paper. Although high-resolution spectroscopy will certainly be a more powerful method for the study of the coronal structuring of active stars than the study of flare decay, the approach used here will still be important in the Chandra -XMM era as it will be applicable to a much larger number of stars (hence spanning a broad range of stellar parameters) than high-resolution spectroscopy. Also, the pressures derived through high-resolution spectroscopy will be weighted by the plasma emissivity and thus, if significant filamentation within loops is present, can in principle be much higher than the average pressure implied by the loop's length and emission measure; such evidence has been reported in the solar case (e.g. Phillips et al. 1996). Therefore, comparison of the spectroscopically measured pressures with the flare-derived emission-measures and lengths will constitute a valuable diagnostic of structuring within a single coronal loop.

Acknowledgements

I am grateful to Ana Maria Garcia Suarez and PhD student Tigran Khanzadyan (Armagh Observatory) for their assistance in the final format of this paper.

11. REFERENCES

1. **Abbett, W.P., & Hawley, S.L.**, 1999, *ApJ*, **521**, 906
2. **Allard, F., & Hauschildt, P.H.**, 1995, *ApJ*, **445**, 433
3. **Andretta, Doyle, J.G., & V., Byrne, P.**, 1997, *A&A*, **322**, 266
4. **Avrett, E.H.**, 1985, *Chromospheric Diagnostic and Modelling, ed. B.W. Lites*, 67
5. **Avrett, E.H., & Loeser, R.**, 1992, *ASP Conference Series*, **Vol.26**, 489
6. **Avrett, E.H., Machado, M.E., & Kurucz, R.L.**, 1986, *The Lower Atmosphere in Solar Flares, ed. D.F.Neidig*, 216
7. **Baliunas, S.L. et al.**, 1983, *ApJ*, **275**, 752
8. **Baliunas, S.L. et al.**, 1995, *ApJ*, **438**, 269
9. **Basri, G., & Marcy, G.W.**, 1994, *ApJ*, **431**, 844
10. **Buchholz, B., Ulmschneider, P. & Cuntz, M.**, 1998, *ApJ*, **494**, 700
11. **Bünte, M., Steiner, O., & Pizzo, V.J.**, 1993, *ApJ*, **268**, 299
12. **Butler, C.J., Rodonò, M., Foing, B.H., & Haisch, B.M.**, 1986, *Nature*, **321**, 679
13. **Byrne, P.**, 1989, *MNRAS*, **255**, 639
14. **Byrne, P., Butler, C.J., & Andrews, A.D.**, 1980, *Ir.Astr.J.*, **14**, 219
15. **Byrne, P., Doyle, J.G., & Menzies, J.W.**, 1985, *MNRAS*, **214**, 119
16. **Byrne, P., & Doyle, J.G.**, 1989, *A&A*, **208**, 159
17. **Carlsson, M.**, 1986, *Uppsala Spec. Rept.*, **N.33**
18. **Carlsson, M., & Stein, R.F.**, 1992, *ApJ*, **397**, L59
19. **Carlsson, M. & Stein, R.F.**, 1997, *ApJ*, **481**, 500
20. **Carmichael, H.**, 1964, *Symp. on the Physics of Solar Flares, NASA SP-50*, 451
21. **Char, S., Foing, B.H., Beckman, J., Garcia Lopez, R.J., & Rebolo, R.**, 1993, *A&A*, **276**, 78
22. **Charbonneau, P., Schrijver, C.J., & MacGregor, K.B.**, 1997, *in Cosmic Winds and the Heliosphere*, 677
23. **Cheng, C.C., & Pallavicini R.**, 1991, *ApJ*, **381**, 234
24. **Cheng, C.C., Oran, E.S., Doschek, G.A., Boris, J.P., & Mariska J.T.**, 1983, *ApJ*, **265**, 1090
25. **Cram, L.E., & Giampapa, M.S.**, 1987, *ApJ.*, **323**, 316
26. **Cram, L.E., & Mullan, D.J.**, 1979, *ApJ.*, **234**, 579
27. **Cram, L.E., & Tod Woods, D.**, 1982, *ApJ.*, **257**, 269
28. **Cuntz, M., Ulmschneider, P., & Musielak, Z.E.**, 1998, *ApJ*, **493**, L117
29. **Donati-Falchi, A., Falciani, R., & Smaldone, L.A.**, 1985, *A&A*, **152**, 165
30. **Doyle, J.G., & Butler, C.J.**, 1985, *Nature*, **313**, 378
31. **Doyle, J.G., & Byrne, P.**, 1986, *A&A*, **154**, 370
32. **Doyle, J.G., Byrne, P., & Menzies, J.W.**, 1985, *MNRAS*, **220**, 223
33. **Doyle, J.G., Houdebine, E.R., Mathioudakis, M. & Panagi, P.M.**, 1994, *A&A*, **285**, 233
34. **Doyle, J.G., Panagi, P.M., & Byrne, P.B.**, 1990, *A&AS*, **228**, 443
35. **Durney, B.R., De Young, D.S., & Roxburgh, I.W.**, 1993, *Sol. Phys.*, **145**, 207
36. **Falchi, A., & Mauas, P.J.D.**, 1998, *A&A*, **336**, 281
37. **Fawzy, D.E., Ulmschneider, P., & Cuntz, M.**, 1998, *A&A*, **336**, 1029
38. **Fisher, G.H., & Hawley, S.L.**, 1990, *ApJ*, **357**, 243
39. **Foing, B.H.**, 1989, *Sol. Phys.*, **121**, 117
40. **Fosbury, R.A.E.**, 1974, *MNRAS*, **169**, 147
41. **Gebbie, K.B., & Steinitz, R.**, 1974, *ApJ.*, **188**, 399
42. **Gershberg, R.E.**, 1974, *Sov. Astron.*, **18**, 326
43. **Giampapa, M.S.**, 1985, *ApJ*, **299**, 781
44. **Giampapa, M.S., Worden, S.P., & Linsky, J.L.**, 1982, *ApJ*, **258**, 740
45. **Gray, D.F.**, 1989, *ApJ*, **347**, 1021
46. **Greiner, J., Duerbeck, H.W., & Gershberg, R.E.**, 1994, *IAU Colloquium 151*, Flares and Flashes

47. Güdel, M., 1997, *ApJ*, **480**, L121
48. Gurzadyan, G.A., 1980, *Flare Stars, Pergamon Press Oxford*
49. Haisch, B.M., 1989, *Sol. Phys.*, **121**, 3
50. Haisch, B.M., Linsky, J.L., Lampton, M., Paresce, F., Margon, & B., Stern, R., 1977,*Ap.J.Lett.*, **213**, L119
51. Haisch, B.M., Strong, K.T., & Rodono,M., 1991, *Ann.Rev.Astron.Astrophys.* , **29**, 275
52. Harper, G.M., 1994, *MNRAS*, **268**, 894
53. Hawley, S.L., & Fisher, G.H., 1992, *ApJS*, **78**, 565
54. Hawley, S.L., & Fisher,G.H, 1994, *ApJ*, **426**, 387
55. Hawley, S.L., & Pettersen, B.R., 1991, *ApJ.*, **378**, 725
56. Hawley, S.L., et al., 1995, *ApJ.*, **453**, 464
57. Hauschildt, P.H., 1992, *J.Quant.Spectrosc.Rad.Transf*, **47**, 433
58. Hauschildt, P.H., 1993, *J.Quant.Spectrosc.Rad.Transf*, **50**, 301
59. Herbold, G., Ulmschneider, P., Spruit, H.C., & Rosner, R., 1985, *A&A*, **145**, 157
60. Hossain, M., & Mullan, D.J., 1993, *ApJ.*, **416**, 733
61. Houdebine, E.R., 1992, *Ir.A.J.*, **20**, 213
62. Houdebine, E.R, Butler, C.J.,Panagi, P.M., Ròdono, M., & Foing, B.H., 1991,*A&AS*, **87**, 33
63. Houdebine, E.R., & Doyle, J.G., 1994a, *A&A*, **289**, 169
64. Houdebine, E.R., & Doyle, J.G., 1994b, *A&A*, **289**, 185
65. Houdebine, E.R., Doyle, J.G., & Koscielecki, 1995, *A&A*, **294**, 773
66. Houdebine, E.R., Mathiudakis, M., Doyle, J.G., & Foing, B.H., 1996, *A&A*, **305**, 209
67. Houdebine, & Panagi, P.M., 1990, *A&A*, **231**, 459
68. Houdebine, E.R, P.M., Ròdono, M., Foing, B.H., 1990, *A&A*, **238**, 249
69. Ionson, J.A., 1984, *ApJ*, **276**, 357
70. Jevremović, 1999, *PhD.thesis*, Queen's University Belfast
71. Jevremović, D., Butler, C.J., & Doyle, J.G., 1998, *ASP Conference Series, Vol.158*, 222
72. Johns-Krull, C.M., & Valenti, J.A., 1996, *ApJ*, **459**, L95
73. Jordan, C., 1997, *Astron. Geophys.*, **38**, 10
74. Joy, A.H., & Humason, M.L., 1949, *Publ.Astro.Soc.Pac.*, **133**
75. Katsova, M.M., 1990, *Sov. Astron.*, **34**, 614
76. Katsova, M.M., & Livshits, M.A., 1991, *Sov. Astron.*, **35**, 65
77. Katsova, M.M., Livshits, M.A., Butler, C.J., & Doyle, J.G,1991, *MNRAS*, **250**, 402
78. Kelch, W.L., Linsky, J.L., & Worden, S.P., 1979, *ApJ*, **229**, 700
79. Keppens, R., MacGregor, K.B., & Charbonneau, P., 1995, *A&A*, **294**, 469
80. Kiepenheuer, K.O., 1964, *Symp. on the Physics of Solar Flares, NASA SP-50*, 323
81. Linsky, J.L., Bornmann, P.L., Carpenter, K.G., Wing, R.F., Giampapa, M.S., Worden, S.P., & Hege, E.K., 1982, *ApJ*, **260**, 670
82. Low, B.D., 1977, *ApJ*, **212**, 234
83. Lu, E.T., & Hamilton, J.R., 1991, *ApJ*, **380**, L89
84. Lu, E.T., Hamilton, J.R., McTieran, J.M., & Bromund, K.R., 1993, *ApJ*, **412**, 841
85. Machado, M.E., & Linsky, J.L., 1975, *Sol.Phys.*, **42**, 395
86. Machado, M.E., Moore, R.L., Hernadez, A.M., Rovira, M.G., Hagyard, M.J., & Smith J.B., 1988, *ApJ*, **326**, 425
87. Marcy, G.W., & Basri, G., 1989, *ApJ*, **345**, 480
88. Martens, P.C.H., & Kuin, N.P.M., 1989, *Sol. Phys.*, **122**, 263
89. Mauas, P.J.D., & Falchi A., 1994, *A&A*, **281**, 129
90. Mauas, P.J.D., & Falchi A., 1996, *A&A*, **310**,245
91. Mauas, P.J.D., Falchi A., Pasquini, L., & Pallavicini, R., 1997, *A&A*, **310**, 245
92. Mauas, P.J.D., Machado, M.E., & Avrett, E.H., 1990, *ApJ*, **360**, 715
93. Montesinos, B. & Jordan, C., 1993, *MNRAS*, **264**, 900
94. Moore R.L., 1988, *ApJ*, **324**, 1132
95. Mould, 1976, *A&A*, **48**, 443
96. Mullan, D.J., & Cheng, Q.Q., 1993, *ApJ*, **412**, 312
97. Øien, A.H., & Alendal, G., 1993, *ApJ*, **412**, 827
98. Pallavicini, R., Tagliaferri, G., & Stella, L., 1990, *A&A*, **191**, 109
99. Pallavicini, R., Tagliaferri, G., & Stella, L., 1990, *A&A*, **228**, 403
100. Panagi, P.M., Byrne, P.B., & Houdebine, E.R., 1991, *A&AS*, **90**, 437
101. Panagi, P.M., & Mathioudakis, M., 1993, *A&AS*, **100**, 343
102. Parker, E.N., 1981, *ApJ*, **244**, 644
103. Parker, E.N., 1983, *ApJ*, **264**, 642
104. Parker, E.N., 1988, *ApJ*, **330**, 474
105. Pettersen, B.R., 1988, *Activity in Cool Star Envelopes, Kluwer Academic Publishers*, 49
106. Pettersen, B.R., 1989, *Sol. Phys.*, **121**, 299
107. Phillips, K.J.H., Bhatia, A.K., Mason, H.E., & Zarro, D.M., 1996, *A&A*, **466**, 549
108. Porter, J.G., Fontenla, A.J.M., & Simnett, G.M., 1995, *ApJ*, **438**, 472
109. Rammacher, W., & Ulmschneider, P., 1989, *in Solar and Stellar Granulation, ed. R.J.Rutten & G.Severino*, 589
110. Raymond, J.C., 1990, *ApJ*, **365**, 387
111. Roberts, B., 1991, *in Advances in Solar System Magnetohydrodynamics, ed. E.R.Priest & A.W. Hood*, 105
112. Robinson, R.D., Carpenter, K.G., & Percival, J.W., 1999, *ApJ*, **516**, 916
113. Rodonò, M., 1986, *The M-type Stars, NASA SP-492*, 409
114. Rosner, R., Musielak, Z.E., Cattaneo, F., Moore, R.L., & Suess S.T., 1995, *ApJ*, **442**, L25
115. Rosner, R., Tucker, W., & Vaiana, G.S., 1978, *ApJ*, **220**, 643
116. Rutten, R.G.M., 1986, *A&A*, **159**, 291
117. Rutten, R.G.M., 1987, *A&A*, **177**, 131
118. Rutten, R.G.M., & Pylyser, E., 1988, *A&A*, **191**, 227
119. Rutten, R.G.M., & Schrijver, C.J., 1987, *A&A*, **177**, 155
120. Saar, S.H., 1994, *IAU Symp. 154, Infrared Solar Physics, ed. D.M. Rabin et al.*, 437
121. Saar, S.H., 1996a, *IAU Symp. 176, Stellar Surface Structure, ed. K.G.Strassmeier & J.L.Linsky*, 237
122. Saar, S.H., 1996b, *IAU Colloq. 153, Magnetodynamic Phenomena in the Solar Atmosphere-Prototypes of Stellar*

MAgnetic Activity, ed. Y. Uchida et al., 367
123. **Saar, S.H., & Schrijver, C.J.**, 1989, *in Cool Stellar Systems, and the Sun V, ed. J.L. Linsky & R.E. Stencel*, 38
124. **Schrijver, C.J.**, 1996, *IAU Symp. 176, Stellar Surface Strucutre, ed. K.G.Strassmeier & J.L.Linsky*, 1
125. **Schrijver, C.J.**, 1987, *A&A*, **172**, 111
126. **Schrijver, C.J., Coté, J., Zwaan, C., Saar, S.H.**, 1989, *ApJ*, **337**, 964
127. **Schrijver, C.J., & Pols, O.R.**, 1993, *A&A*, **278**, 51
128. **Simon, T. & Drake, S.A.**, 1989, *ApJ*, **346**, 303
129. **Skumanich, A.**, 1985, *Austr.J.Phys.*, **38**, 971
130. **Steinolson, R.S., & Davila, J.M.**, 1993, *ApJ*, **415**, 354
131. **Steiner, O., Grossmann-Doerth, U, Schüssler, M., & Knölker, M.**, 1996, *Sol.Phys.*, **164**, 223
132. **Steiner, O., & Pizzo, V.J.**, 1989, *A&A*, **211**, 447
133. **Stern, R.A., Schmitt, J.H.M.M., & Kahabka, P.T.**, 1995, *ApJ*, **448**, 683
134. **Strassmeier, K.G., Handler, G., Punzen, E., & Rauth, M.**, 1994, *A&A*, **281**, 855
135. **Sturrock, P.A., Kaufman, P. Moore, R.L., & Smith, D.F.**, 1984, *Sol. Phys.*, **94**, 341
136. **Sturrock, P., et al.**, 1986, *Physics of the Sun Vol.2*
137. **Ulmschneider, P., & Musielak, Z.E.**, 1998, *A&A*, **338**, 311
138. **Ulmschneider, P., Musielak, Z.E., & Fawzy, D.E.**, 2000, *A&A*, in preparation
139. **Ulmschneider, P., Theurer, J., & Musielak, Z.E.**, 1996, *A&A*, **315**, 212
140. **Ulmschneider, P., Zähringer, K., & Musielak, Z.E.**, 1991, *A&A*, **241**, 625
141. **Uitenbroek, H.**, 1989, *A&A*, **213**, 360
142. **Valenti, J.A., Marcy, G.W., & Basri, G.**, 1995, *ApJ*, **439**, 939
143. **van Ballegooijen, A.A, & Mertens, P.C.H.**, 1989, *ApJ*, **343**, 971
144. **Ventura, P., Zeppieri, A., Mazzitelli, I., & D'Antona, F.**, 1998, *A&A*, **331**, 1011
145. **Vernazza, J.E., Avrett, E.H., & Loeser, R.**, 1981, *ApJS*, **45**, 635
146. **Walter, F.M.**, 1996, *IAU Symp. 176, Stellar Surface Structure, ed. K.G. Strassmeier & J.L.Linsky*, 355
147. **Young, A., Skumanich, A., & Harlan, E.**, 1984, *ApJ*, **282**, 683
148. **Zirin, H.**, 1988, *Solar Astrophysics. Cambridge University Press*